Second Semi-Annual Progress Report

on

DYNAMICS AND CONTROL OF ESCAPE AND RESCUE FROM A TUMBLING SPACECRAFT

(1 December 1971 to 31 May 1972)

NASA Grant NGR 39-009-210

Principal Investigator

Marshall H. Kaplan

Associate Professor of Aerospace Engineering

The Pennsylvania State University

University Park, Pa. 16802

Submitted to:

National Aeronautics and Space Administration

Washington, D. C. 20546

June 1972

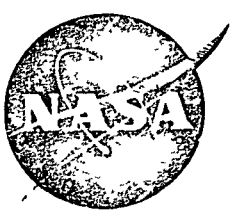

TABLE OF CONTENTS

I. INTRODUCTION

The subject grant (NGR 39-009-210) on the dynamics and control of escape and rescue from a tumbling spacecraft was initiated on 1 June 1971. This is the second semi-annual status report. During the past six months (1 December 1971 to 31 May 1972) tasks which were initially outlined in the first status report (December 1971) have been continued. Accomplishments are cited and future plans listed. Individual personnel assignments are also cited. Detailed descriptions of accomplishments are left for appendices while a short summary of each is offered in Section III.

The problem of escape and rescue has been attacked primarily from the point of view of controling vehicle motion before crew rescue can be affected. Thus, task assignments have been oriented toward devices and techniques associated with active and passive detumbling. As these are completed the problems of crew escape from a tumbling vehicle will be considered.

Communication and dissemination of results is considered a primary part of university research. Thus, interaction with industry and NASA on this work has been actively sought. Three representatives from Penn State, including the principal investigator, attended the final review briefing of a North American-Rockwell contract (NAS 9-12004), "Safety in Earth Orbit Study", on 2 June 1972 at NASA MSC. Specific comments were offered on the use of fluids for detumbling, general attitude motion, and detumbling processes. A summary of work to date will be presented as a paper entitled, "Despinning and Detumbling Satellites in Rescue Operations," at the Fifth International Symposium on Space Rescue in Vienna, October 1972. Although this

paper is not yet completed, an abstract is included here as Appendix A.

II. PERSONNEL

Although the grant budget provides support for two graduate assistants, there are currently three graduate students and one undergraduate working on related tasks. Two are supported by the grant (T. Edwards and J. Stimpson), while the third graduate is a NSF Trainee (B. Kunciw). The undergraduate (W. Snow) is studying an automatic docking and detumbling device for his Senior Research Project and will continue on this as a graduate student beginning Summer Term 1973. All three current graduate assistants will receive advanced degrees (2 M.S. and 1 Ph.D.) during the second year of this grant. Each of their theses will be published as an Aerospace Engineering Report as well as appear in article form in appropriate journals.

In addition to continuing personnel, Dr. W. M. Phillips consented to provide material on the use of fluids for application to detumbling torques. Both gases and liquids were considered and results of his investigation are included here. Dr. Phillips, Assistant Professor of Aerospace Engineering, has done a great deal of analytical and experimental research on the properties of fluid jets into a vacuum.

III. PROGRESS TO DATE

Basic task assignments presented in the first status report (December 1971) have not changed significantly. However, as progress

is made, interactions and objections must be modified to reflect the current and expected situation. Therefore, a new project flow chart has been constructed showing specific areas of study for the next year. This is presented in Figure 1. Individual efforts are briefly discussed below.

A primary requirement for external detumbling a passive space base is the application of torque. The use of fluids avoids "hard docking" by the rescue vehicle and permits variable torque applications. However, the properties of large liquid jets in vacuum are not well known. Feasibility of using gas and liquid jets has been considered. It was concluded that the gas jet can only be used to provide a gaseous cloud which would be effective as a drag source for general energy dissipation. This results in long detumble times and low utilization efficiencies. The liquid jet appears more attractive, because it can be directed. However, the lack of knowledge about jet spreading and ice formation indicates that considerable experimentation with water and other liquids is necessary to determine feasibility. Detailed discussion and analysis are presented in Appendix B.

An alternative method for external detumbling is an unmanned module or "anti-tumbling space vehicle"* which can follow and hard-dock with the distressed vehicle. The worst case tumbling analysis, appearing in the last status report, indicated that tumbling rates would be low enough to permit a small device to track and dock with

---

* First suggested by J. W. Wild and H. Schaefer in "Space Rescue Operations," presented at the 3rd International Symposium on Space Rescue, Constance, Germany, October 1970.

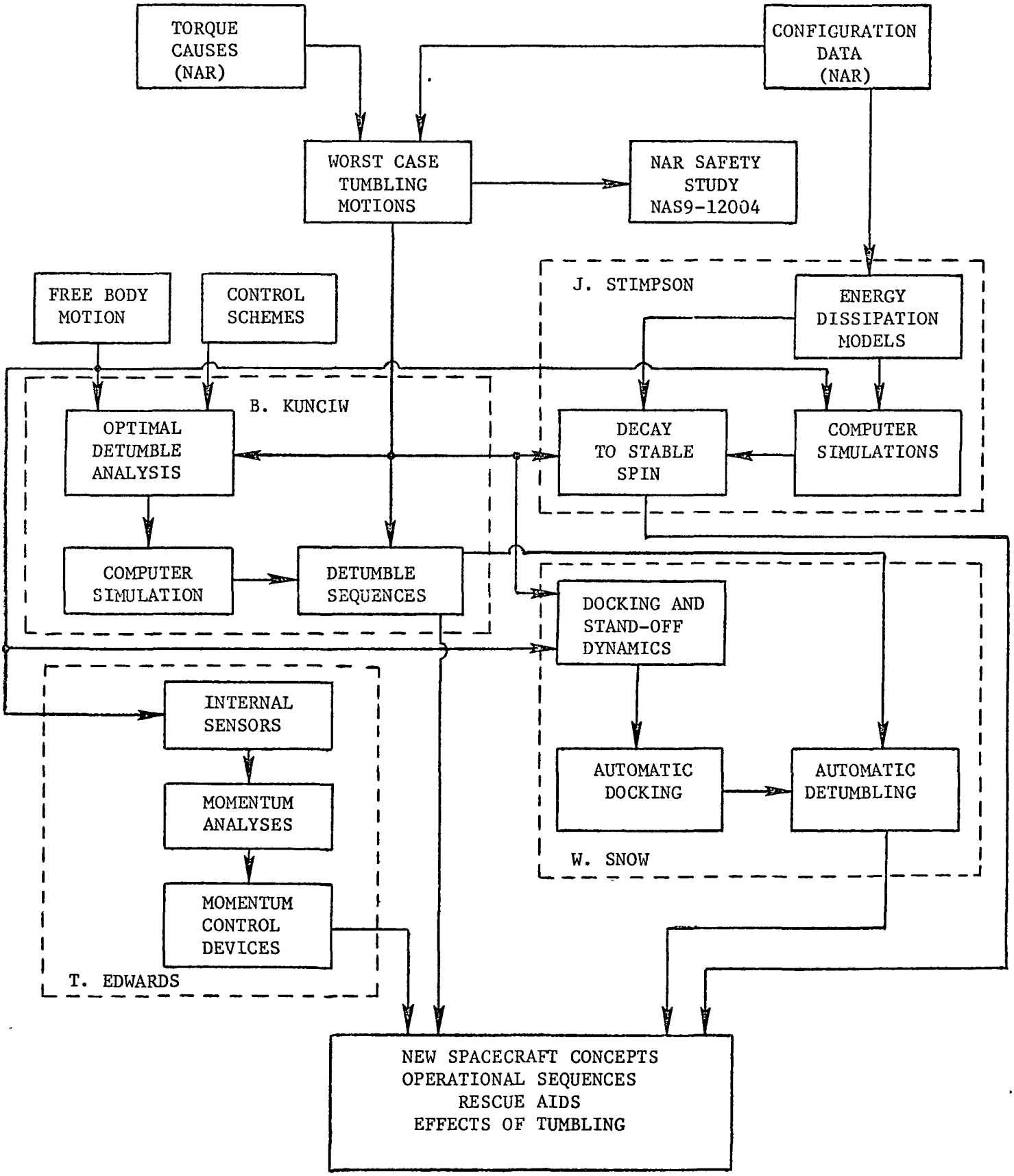

Figure 1 Project Flow Chart

a larger vehicle. A conceptual design of such a device has been formulated. The Module for Automatic Dock and Detumble (MADD) is highly maneuverable and self-contained. Preliminary analyses related to the dynamics and control of such a device have been carried out. Position and attitude control systems for various phases of operation have been synthesized along with an operational procedure. Sequence of events consists of rendezvous from the shuttle orbiter, pacing a docking position, docking, and detumbling. Detailed description and control analyses of MADD are presented in Appendix C.

The time to perform the detumbling operation may be critical for crew survival. Therefore, it is very desirable to execute this maneuver in minimum time. This problem of optimally detumbling a space vehicle assuming reaction jets are actively available on the distressed vehicle has been investigated. Such jets would be built into a MADD device for use after docking. This problem of minimum time detumble may be separated into two branches based on the type of reaction jet control available: (1) with a constraint on the magnitude of the control moment vector, (2) with constraints on the magnitude of each of the three components of the control moment vector. The choice of constraint for actual rescue missions will depend on cost and complexity of a detumbling module. Solution of the minimum time problem with a constraint on magnitude of the control moment vector is relatively straightforward; the required control moment vector is directed opposite to the angular momentum vector and has the largest magnitude that the reaction jets can supply. Using this technique, the modular space station (MSS) tumbling at 1.150, 1.750 and -0.445 RPM about the 1,2 and 3 principal

axes, respectively, was brought to near zero angular velocity in about 7 minutes with the application of a maximum torque magnitude of 2500 ft-lbs. Equations governing minimum time detumbling of a distressed vehicle using the second constraint (i.e., constraints on the magnitudes of each of the three components of the control moment vector) have been obtained; these equations require 3 on-off control moments of fixed magnitude. However, the mathematics for the determination of switching times for this nonlinear minimum-time problem still have to be developed. Analyses and mathematical development associated with optimal detumbling are discussed further in Appendix D.

To this point active external torquing devices and methods have been discussed exclusively. Another approach to detumbling is through the use of internal passive and active devices. Mass expulsion and momentum exchange are two typical examples of active control techniques. Programmed movement of a large internal mass to control moments of inertia is a possibility for use in stabilizing tumbling to steady spin. Dampers, fuel slosh, and structural flexibility are examples of passive energy dissipation mechanisms which lead to minimum-energy, steady-spin about the major principal axis of the distressed vehicle. Such passive mechanisms are typically very slow in stabilizing tumble. However, these may be enhanced by pre-installed devices. Initial studies are concerned with detumbling effects of structural flexibility on free-tumbling motion. Appendix E presents a survey of methods for analyzing flexibility effects and discusses the formulation of interest here. Appendix F discusses active internal control techniques and identifies methods of analysis for devices of interest.

IV. FUTURE TASKS

Efforts will continue in the areas of optimal detumble analyses, automated dock and detumble devices, and internal active and passive schemes. Of particular concern will be the MADD concept. Further work will be done on the dynamics of stationkeeping with a tumbling vehicle and associated autopilots. Simulations of such operations will be carried out with the aid of computers. These tasks should lead to a more refined design for MADD.

The problem of minimum time detumbling with constraints on the magnitude of each torque component will be investigated further. Control torques must be the on-off or "bang-bang" type. However, an exact switching time analysis is required. Several methods of solving this problem have been considered; including steepest descent, linear programming, and successive sweep techniques. Steepest descent is advantageous since it is quite insensitive to initial choice of control. Its major disadvantage is slow or no convergence to an accurate solution. The successive sweep method is not well suited to the detumbling problem since it is very sensitive to the initial guess for the control history. However, these two methods could be used together. The former would give a near optimal path and the latter would refine it to obtain an optimal solution. A more straightforward approach might be a linear programming method. The use of linear programming to solve non-linear control problems has lead to effective solutions for minimum fuel attitude maneuvers. This method is relatively insensitive to the nominal control history and converges quickly. Furthermore, it takes advantage of linear

programs for digital computers already available. Therefore, this method will be given priority.

Studies of internal active and passive stabilizing techniques will continue. Flexibility effects will be modelled for specific cases and results developed into general implications for this problem. Initially, a simplified model of a nonrigid spacecraft will be studied to determine interactions with tumbling motion. Stabilizing effects will then be investigated to estimate the time to reach a steady spin state. Efforts on active internal control will be directed toward analyses of possible candidate devices, such as moving masses, momentum wheels, and reaction jets. Computer simulations will be required to evaluate these possibilities.

Further interaction with industry and NASA is continually sought. Opportunities to participate in space safety activities with contractors are always of mutual benefit from both an education and research point of view. Dissemination of results and participation in conferences and seminars is a major objective of such research grants.

APPENDIX A

Abstract for Fifth International Space Rescue Symposium
(Vienna, Austria, 10 October 1972. To be held in conjunction
with the 23rd I.A.F. Congress, 8-13 October 1972)

DESPINNING AND DETUMBLING SATELLITES IN RESCUE OPERATIONS*

by
Marshall H. Kaplan
Department of Aerospace Engineering
The Pennsylvania State University
University Park, Pennsylvania, U.S.A.

ABSTRACT

In the operation of manned space bases of the future, there is always a finite probability that an accident will occur and result in uncontrolled tumbling of a vehicle. Therefore, an escape and rescue capability for such situations is highly desirable. The process of detumbling the spacecraft may represent a major part of the operation, since the elimination of angular motion of a large tumbling body presents a very difficult problem which must be resolved in order to fulfill a complete space rescue capability.

The most general type of passive attitude motion is referred to as "tumbling," because all three orthogonal components of angular velocity may be large and there is no preferred axis of rotation. Since no spacecraft is absolutely rigid, tumbling motion will tend toward steady spin due to energy dissipation. However,

*This work is being supported by NASA Grant NGR 39-009-210.

large bodies such as space stations have relatively low dissipation rates and may require many weeks to passively stabilize. This paper discusses the operational aspects of rescue from a tumbling or spinning vehicle and presents techniques for detumbling or despinning such craft.

APPENDIX B

Use of Fluids for the Application of Detumbling Torques

(W. M. Phillips)

I. Gas Jets

Discussion

An ideal gas exhausting into vacuum produces an exhaust plume of ever decreasing "cell" size until viscous dissipative effects wash out the signature. The plume is usually highly expanded, producing a shock structure. However, in space (the absence of all background molecules) there is little opportunity for significant shock structure. One simply produces a highly expanded exhaust cloud.

The problem should be considered on two fronts. In the first case one considers the utilization of the exhaust from some available propulsion system. In this mode one must deal with hot exhaust gases, perhaps some particulate matter, and a highly expanded plume. In the second case one invisions utilization of a "carry on" gas system. This latter mode has the advantage of controlled expansion (through a nozzle) to lower exhaust pressures. The difficulty is the time scale for significant momentum transport to an external vehicle if the exhaust plume is expanded to the ideal near ambient environment. This would

require low source pressures or an enormous exhaust nozzle. (See for example Ref. 1 for an exit pressure to background ratio of 10^6. The plume is expanded through 122°.)

To illustrate the basic features of gas exhaust into space, two examples are given.

Case 1:

Assume a continuum expansion (somewhat unrealistic but the best possible case) to an exit pressure, $p_E \simeq 0(0)$. The momentum transfer will be

$$F = \rho u^2 A$$

where ρ = density and u is the gas velocity. The exhaust velocity can be estimated from an adiabatic expansion to a static temperature, $T_\infty \sim 0$ as

$$C_p T_o = \frac{U^2}{2}$$

or

$$u^2 \simeq 2C_p T_o$$

where C_p is the constant pressure specific heat and T_o is the source or stagnation temperature. For expansion into vacuum it is easy to attain velocities of this order of magnitude.

The simplest case is Newtonian drag on the vehicle. The drag coefficient is

$$C_D \sim 2\sin^3\alpha$$

The maximum drag is

$$\text{Drag} = C_D \rho u^2 A/2$$

since for normal impingement

$$\alpha = 90°$$

$$\frac{\text{Drag}}{\text{Area}} = \rho u^2$$

$$\frac{\text{Drag}_{max}}{\text{Area}} = \rho u_{max}^2$$

$$\frac{D_{max}}{\text{Area}} = 2 \sum_i n_i m_i \overline{C_{p_i}} T_o$$

where i is a summation over the species present in the exhaust plume. Therefore one simply selects the species of gas, the source temperature attainable, $\overline{C_p}$ and the number density for required momentum transfer is given.

The number density, n(x) in an exhaust plume is

$$\frac{n(x)}{n_o} \sim \frac{1}{r^2}$$

where n_o is the source density. For a simple gas

$$n(x) \sim 0.161 \left(\frac{d}{x}\right)^2 n_o$$

At 200 nozzle diameters downstream

$$n(x) \sim 0(0.1) \frac{1}{4} \times 10^{-4} n_o$$

or

$$n(x) \sim 2.5 \times 10^{-6} n_o$$

while the constant would vary with the species, the order 10^{-6} is realistic

$$\frac{D_{max}}{Area} \sim (2 \times 10^{-6})\ \rho_o\ \overline{C_p}\ T_o$$

Assuming $\rho_o \sim 0\ (\frac{p_o}{RT_o})$

$$\frac{D_{max}}{Area} \sim 2 \times 10^{-6}\ p_o\ \frac{\overline{C_p}}{R}$$

The source pressure p_o and the source gas constant then fix the drag value.

Case 2:

Assume for a moment that the exhaust plume of a vehicle is to be utilized for this purpose.

a. For a typical rocket exhaust nozzle operating at 60 miles altitude the exhaust plume is expanded about 150 nozzle exit radii at a distance of about 130 nozzle radii down stream (Ref. 2) (For example a 1 ft. nozzle would have a 300 foot diameter plume at 130 feet downstream.) In this mode one must simply invision detumbling by drag in the exhaust cloud.

At the present time it is difficult to predict the diffusive dissipation of such an exhaust cloud without experiment. (An experiment of this type has been proposed for the space shuttle program.) The local static pressure in the cloud can be estimated at <u>130 feet</u> from a 1 foot exhaust nozzle. Reference 2 gives

$$p_{\substack{max \\ 130\ ft.}} \sim 1 \ \ lbf/ft^2$$

for a source pressure, p_o of 125 psia

$$P_{\substack{max \\ 45\ ft.}} \sim 5 \ \ lbf/ft^2$$

Since one cannot aim such a jet at the proper area for detumbling (and therefore gain from impact or total pressure recover), the static pressure is the best estimate available. The invisid prediction would give a Mach number of $O(20)$ and

$$\frac{p_{static}}{p_o} \sim \left(1 + \frac{\gamma - 1}{2} M^2\right)$$

$$\frac{p_{static}}{p_o} \sim 2 \times 10^{-7}$$

$$p_{static} \sim (2 \times 10^{-7})\ (125)\ (12) = 3000 \times 10^{-7}$$

$$p_{static} = 3 \times 10^{-4} \ lbf/ft$$

This is considerably less than the experimental value since the latter includes at least part of the dynamic component.

Conclusions

At a distance of 200 ft a gas exhaust plume will be greatly expanded and any tumbling vehicle would most likely experience a gas cloud with resulting drag due to environmental particle density rather than directed jet impact. One cannot invision aiming such

an exhaust at part of the vehicle. The number density at 200 feet would be greatly reduced and this mode would require a considerable source pressure to work at all. The exhaust plume would dissipate under diffusion. This is of concern since the time scale for detumbling by this mode is necessarily large. The method might require quasisteady exhausting to be effective and this would require a large source capability. The method is not considered feasible due to these aspects and the order of magnitude analysis previously discussed. While admittedly one can compute slight improvements by changing gas species and nozzle design or approaching the tumbling vehicle more closely, these gains would be slight. It is felt that effort is better expanded elsewhere.*

II. Liquid Jets

Discussion

The use of a liquid stream ejection method to control or arrest tumbling has the following attractive features:

(a) It may be directed if the jet angle can be kept small.

(b) It is remote with no dangerous feedback to the rescue vehicle.

(c) It is inexpensive, disposable and reliable.

While it is difficult to predict the far field nature of the jet in detail, the following observations can be made:

---

*It should be noted that no experimental information is available. on the dissipation of exhaust gas clouds in space precluding definite conclusions here. Furthermore, due to contamination level requirements with missions such as invisioned with the space shuttle, this information should be experimentally obtained and theoretical estimates checked.

(1) The nature of the jet
   a. Viscosity - an increased viscosity results in a more compact jet and larger droplet size
   b. Surface tension - same result
   c. Nozzle geometry - length/diameter should be optimum for jet compactness - difficult to assess
      polish - high polish required to maintain low turbulence and reduce jet spread
      diameter - larger orifice diameter results in less jet spread over the same axial distance
   d. Turbulence - higher Reynolds number will result in faster jet spread
   e. Injection pressure - higher I.P. results in greater jet core angle

(2) Phase
   a. Atomization and expansion into space will likely result in ice particles. Furthermore, the pressure will be below the vapor pressure of ice (4.579 mm Hg at 0° C). Rate of ice formation and sublimation will depend on the droplet size (determined by atomization). Expect more spread than with liquid jet.
   b. Water - evaporation will take place at a rate dependent on droplet size.

Analysis

A. Exit Conditions

The effects of exit Reynolds number can be seen in Figures 2 and 3. It is obvious that a low exit Reynolds number is desirable to minimize the jet angle far downstream. Turbulence (which will increase spread) is determined by the exit conditions. However, a low exit Reynolds number is inconsistent with large impact force per unit area at a great distance from the nozzle exit. (The working condition of 200 ft distance is a large distance for these considerations).

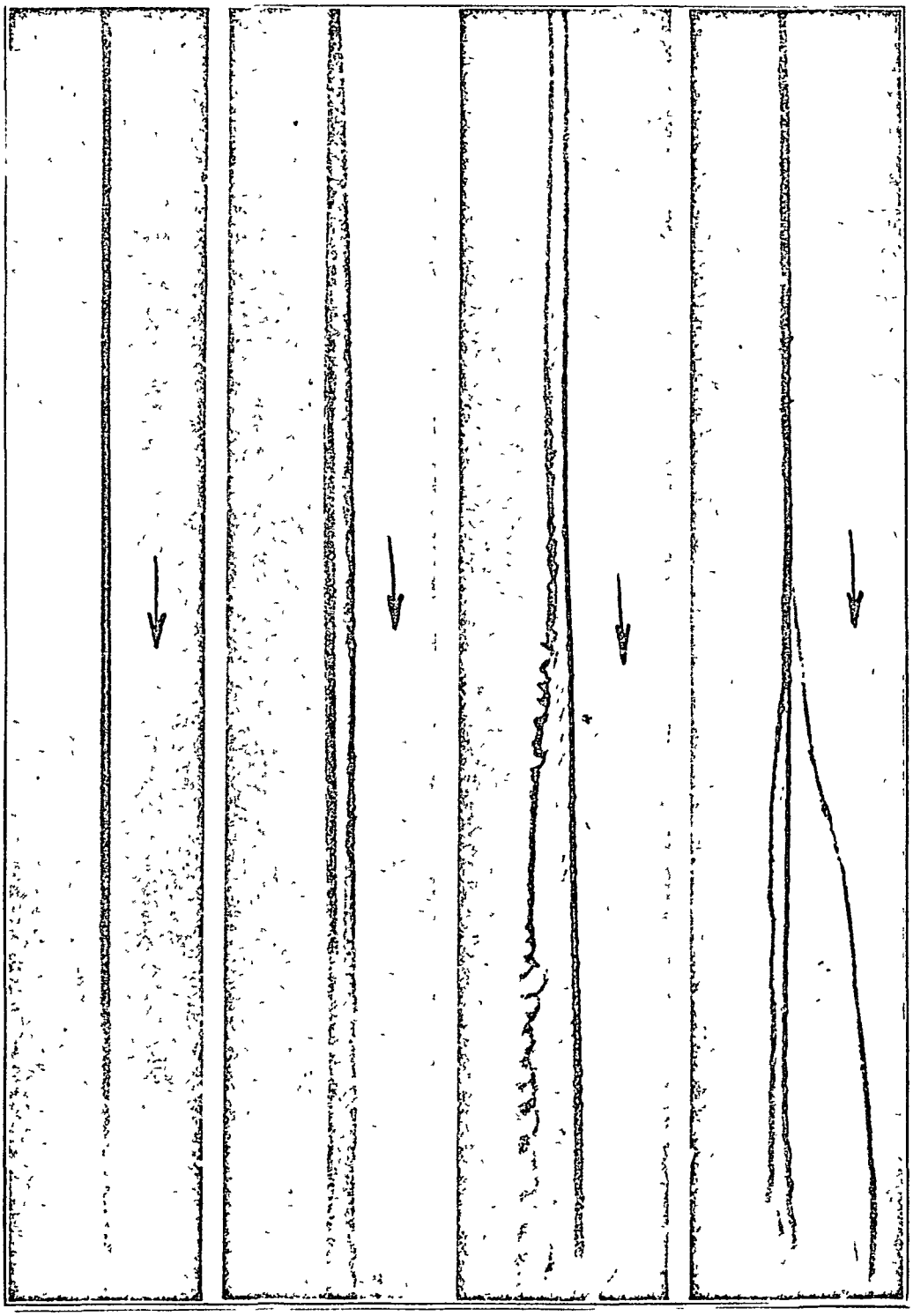

R N = 1,500 R N = 2,400 R N = 2,600 R N = 3,000

FIGURE 3.- Fuel jets at various Reynolds Numbers, in vacuum, × 2 5 Orifice diameter, 0 020 inch, air density, 0 0013 atmosphere (pressure = 1 mm Hg, absolute), fuel viscosity, 0 102 poise at 22° C , photographs taken just beyond the orifice

R N =3,500 R N =5,000 R N =7,000 R N =9,000

FIGURE 3—Fuel jets at various Reynolds Numbers, in vacuum, × 2 5 Orifice diameter, 0 020 inch, air density, 0 0013 atmosphere (pressure = 1 mm Hg, absolute), fuel viscosity, 0 102 poise at 22° C , photographs taken just beyond the orifice 3

For example:

	Case 1	Case 2
Source Pressure	70 lbf/in^2	1100 lbf/in^2
Jet Velocity	100 ft/sec	400 ft/sec
Nozzle Area	0.05 cm^2	10 cm^2
Nozzle Radius	0.126 cm	1.78 cm
Distance	200 ft	

Assuming that the jet can be maintained laminar the jet angles can be estimated. The jet is ideally represented in Figure 4. Referring to the geometry,

$$\tan \theta_i = \frac{r_I - r_n}{\ell}$$

then

Case 1: $\tan \theta_{i_{min}} = 0.00885$; $\theta_{i_{min}} = 0.5°$ and

$A_{impact} = 10 ft^2$

Case 2: $\tan \theta_{i_{max}} = 0.0282$; $\theta_{i_{max}} = 1.6°$ and

$A_{impact} = 100\ ft^2$

However, the exit Reynolds number in case 1 is 40,000 indicating that the jet would not be maintained as shown.

The effects of exit geometry are illustrated in Figure 5 and discussed in Ref. 3. Again we see that the jet spread is sensitive to exit geometry. It is obvious that experimental results

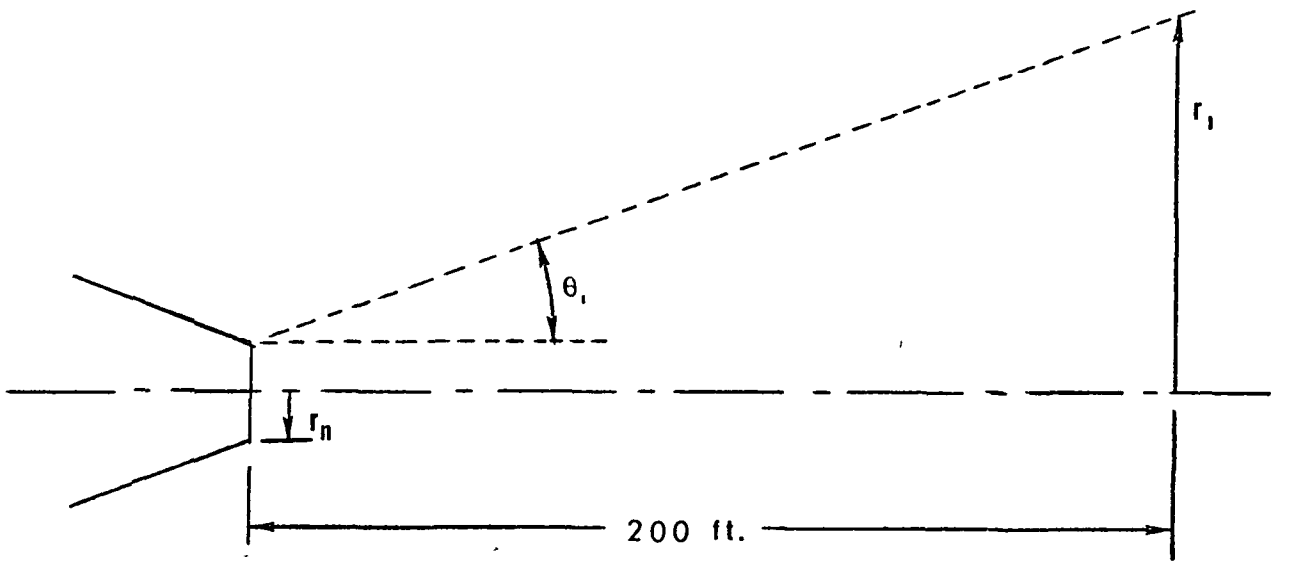

Figure 4. Liquid Jet Signature

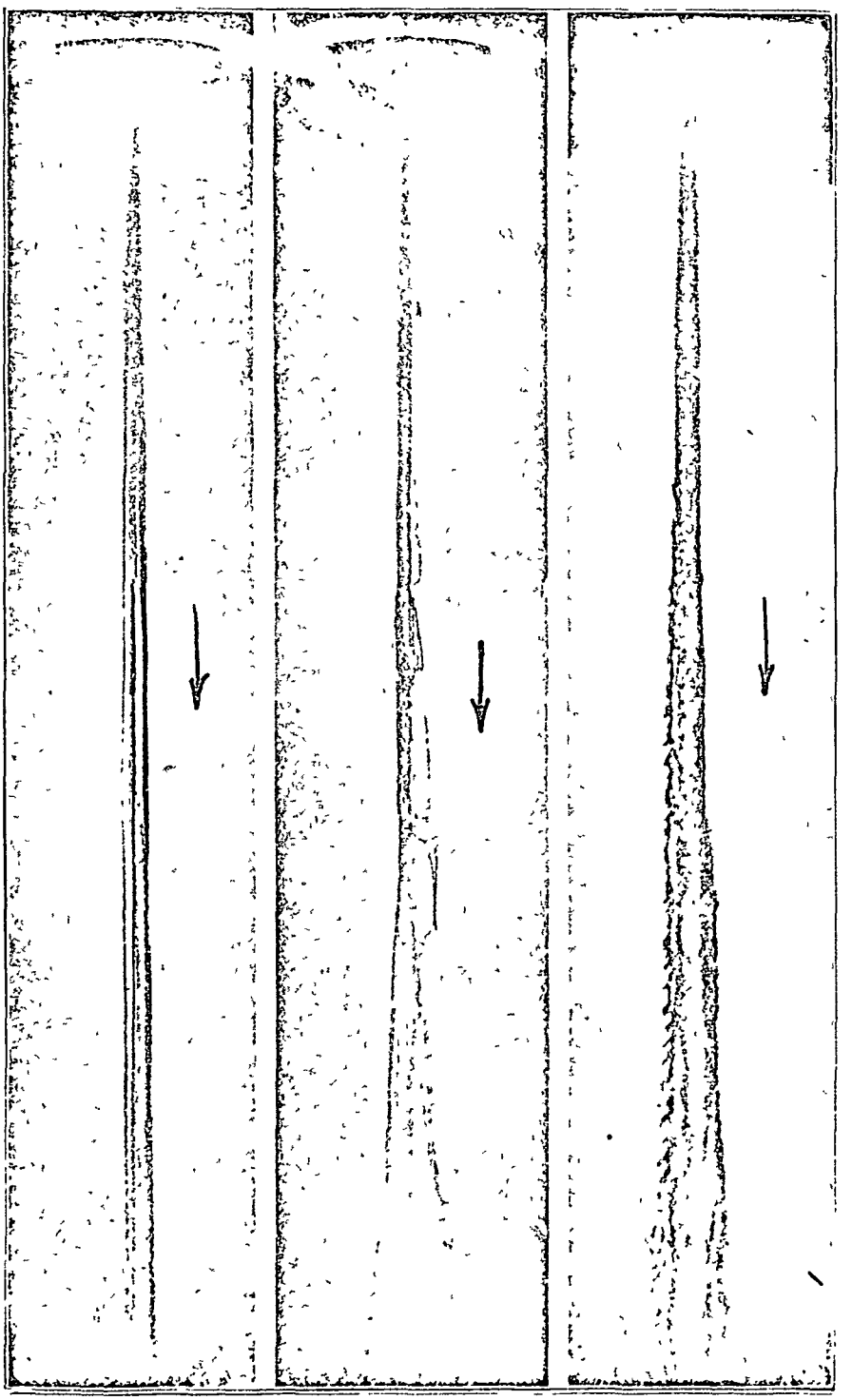

(a) (b) (c)

FIGURE 5 Jets from orifices having the same dimensions, in vacuum, × 2 5 Injection pressure, 3,000 pounds per square inch, orifices, 0 014 inch in diameter and 0 028 inch long, air density, 0 0013 atmosphere (pressure=1 mm Hg, absolute)[3]

Nozzles·

(a) straight hole in thin steel plate. (b) conventional nozzle, polished (c) conventional nozzle, unpolished

are essential since such effects cannot be predicted otherwise. In fact there is little or no data whatsoever on liquid jets exhausting into space. One must inspect carefully all results from vacuum chamber since minute traces of gas can be catastropic to jet continuity at large distances. However, this mode can only be adequately examined in that manner.

B. Composition

The liquid jet fluid should have:
high viscosity
high surface tension
low vapor pressure
high molecular weight

Conclusions

(1) The jet spread will be greater than predicted

(2) If atomized and ice crystals are formed, the conclusion that localized impingement pressures are reduced is false unless the particles are very small. (Something can be gained by minimizing the particle size since the impact pressure $\propto$ mass $\propto r^3$ while the impact area of particle $\propto r^2$.) However, one still worrys about a spacecraft designed for operation under no drag now operating in a hailstorm.

(3) Considerable experimental results would be necessary to predict jet characteristics to prove feasibility.

(4) Fluids other than water should be considered to take advantage of the characteristics noted in A as well as to gain the advantages of a lower freezing point and lower vapor pressure.

III. Summary

The gas jet and water jet have been examined as possible modes for detumbling a space vehicle. While both methods are somewhat inefficient, a catastrophically tumbling vehicle might

indicate such an approach. In this event, the fluid jet seems perferable due to the larger momentum transfer possible over shorter time scales. The success of such a process, however, is dependent on nozzle design, fluid employed, etc., and many of these features can only be optimized by experiment. Finally, further examination is required to estimate the formation of solid particles (ice) and their possible destructive influence on the vehicle undergoing rescue.

IV. References for Appendix B

1. Andrews, E. H., Vick, A. R., and Craidon, C. B., "Theoretical Boundaries and Internal Characteristics of Exhaust Plumes from Three Different Supersonic Nozzles," NASA TN D-2650, 1965.

2. Wayte, M. J. et al., "A Study of Rocket Exhaust Plumes at High Altitude," AIAA Paper 69-575, AIAA 5th Propulsion Joint Specialist Conference, 1969.

3. Lee, D. W. and Spencer, R. C., "Photomicrographic Studies of Fuel Sprays," NACA Rept. No. 454, 1933.

APPENDIX C

Module for Automatic Dock and Detumble (MADD)

(W. Snow)

NOMENCLATURE

f_i = Control acceleration about subscripted axis (i = x,y,z)

I_i = MADD moments of inertia about subscripted axis (i = x,y,z)

I_i = MSS principal moments of inertia about subscripted axis (i = 1,2,3)

L_i = Disturbance torque about subscripted axis (i = x,y,z)

m = Maximum allowable applied moment

m_i = Control torque about subscripted axis (i = x,y,z)

p,q,r = Angular velocities of MADD

u_i = Control variable about subscripted axes (i = 1,2,3)

X,Y,Z = Moving coordinate frame

X',Y',Z' = MSS body fixed coordinate frame

x,y,z = Right hand coordinate frame

δ = Gimbal angle

Ω = Gyro angular velocity

ω_i = MSS angular velocities about subscripted axis (i = x,y,z)

ω_i' = MSS angular velocities about subscripted axis (i = x',y',z')

ϕ,ψ,θ = Euler angles for a right hand system

I. Introduction

In the operation of a large modular space station (MSS) there is a small but finite probability that an accident will render it disabled and tumbling. The MSS must be detumbled before evacuating the crew and repair of the control systems can be performed. Tumbling is a result of a significant attitude perturbation of an uncontrolled MSS. This results in continuous angular motion about all three principal body axes, i.e., no inertially oriented axis. The MSS would reach a stable spin after a sufficient amount of energy was dissipated, but this might take many weeks or months. Astronauts trapped in the tumbling MSS could not easily escape.

Situations that are most likely to cause tumbling of the MSS are collision, malfunctioning thruster, and escaping stored gas or liquid. From a worst case analysis, tumble rates are as high as 2 RPM about the principal axes for the cases mentioned above.[1]

Elimination of angular motion must be done from the non-tumbling frame of the shuttle. A Module for Automatic Dock and Detumble (MADD) could perform an orbit transfer from the shuttle and then a docking maneuver with the MSS. Once docked MADD could apply torques by firing its thrusters to detumble the MSS. This could be done in a time optimal manner. Once the MSS is detumbled, the crew can be rescued and the mission completed.

II. Description of MADD

The purpose of MADD is to detumble a passive modular space station. It will be assumed that the MSS will be tumbling at an equivalent 2 RPM or less with no inertially oriented axis.

The design of MADD is influenced by mission objectives, and system constraints. The vehicle must be able to maneuver to, dock with, and detumble the MSS with a limited amount of fuel for various tumbling situations. The size of MADD is constrained by the need for maneuverability and the size of the shuttle cargo bay dimensions, which are proposed to be 15 ft in diameter by 60 ft in length. The size is also dependent upon the sizes of docking ports on the MSS.

It is necessary that the CM of the MADD remains fairly well fixed as fuel is consumed to simplify control requirements. Therefore, the fuel tanks should be evenly distributed about the center of mass. Thrusters should be far enough from the CM to minimize attitude thrusting during transfer, but not so far as to put excessive moments on the docking mechanism during detumbling. MADD must have full orbit and attitude control for transfer to the MSS. A preliminary configuration for MADD, based on these considerations is shown in Figures 6 and 7.

The structure of this vehicle contains all subsystems with the docking probe mounted beneath and docking drogue mounted above the main structure, which is a 9 ft octagon and 4 ft deep.

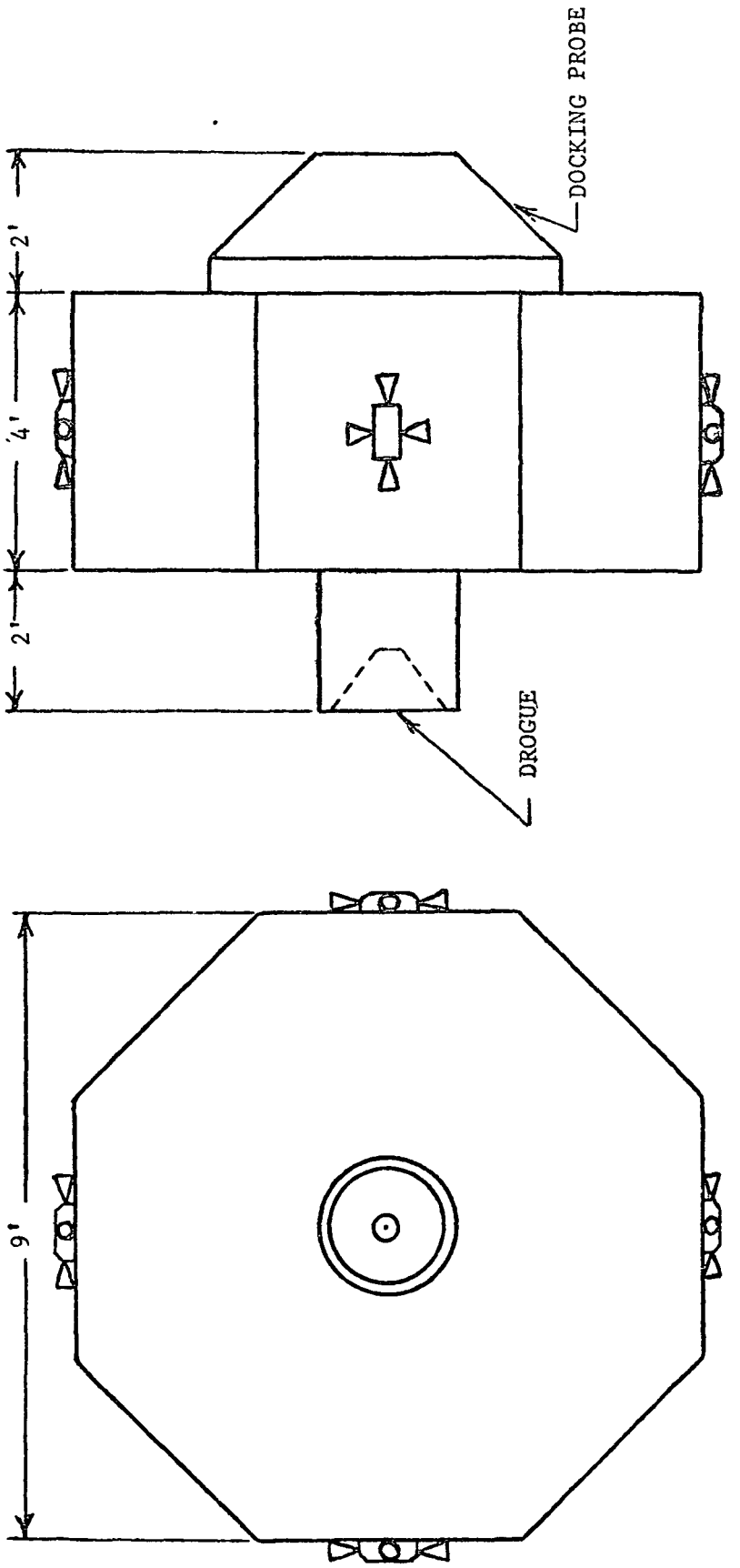

Figure 6 Details of MADD Configuration

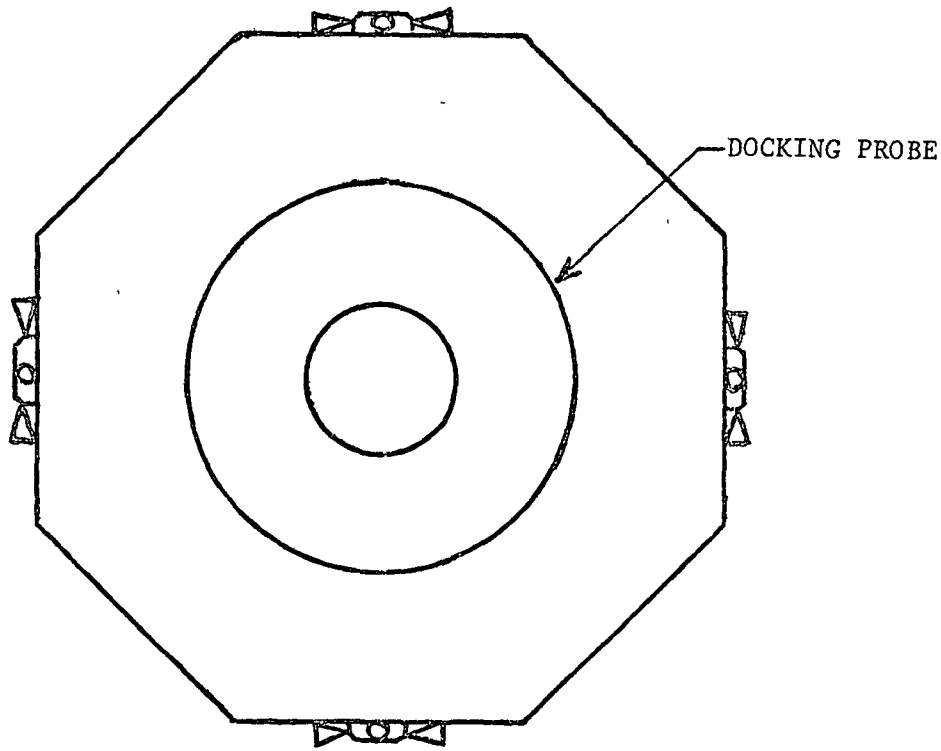

Figure 7 Details of Docking Probe Configuration

This contains hydrazine storage tanks, control systems, batteries, and twin gyro attitude controllers. Subsystems are categorized as: structure, computer, command and telemetry, power supply, control systems, and docking apparatus. The power supply will consist of storage batteries.

The control systems consist of three units: position, attitude, and detumble. The position and attitude control systems, after being programmed by the shuttle, provide maintenance of orientation and position during transfer and docking. Twin-gyro torquers were chosen for the attitude control. Monopropellant hydrazine thrusters were chosen for position control, detumbling, and momentum dumping. Hydrazine was chosen for efficiency, easier handling, and lower operating temperature than that of a bipropellant.[2] During detumbling of the MSS, the twin-gyros will be locked. Once the MSS is detumbled, the twin-gyros may be given new reference signals and released. Also during detumbling, the position control system may be reactivated upon command of the shuttle.

Thrusters used for position control are also used for detumbling the MSS and attitude control. This was done to eliminate the need for three separate systems of thrusters, even though three separate control systems control the thrusters. The thrust profile during the detumbling procedure is computed by an on-board computer according to results of the optimum detumbling analyses.

The docking apparatus consists of two separate systems; one for the MSS and one for the shuttle. MADD docking probe is assumed to dock with one of the docking ports located at the extremities of MSS modules. The capture latches are activated by MADD after alignment. The shuttle docking system consists of docking arm, probe, capture latches, and a docking drogue, which is activated by the shuttle crew. Crew positions MADD above the shuttle as illustrated in Figure 8. It is then released to perform the mission afterward, the docking arm is extended from the cargo bay until the capture latches are aligned with the drogue and MADD can be stowed for reuse later.

III. Operational Procedure

Rescue operations begin as the shuttle completes its rendezvous with the MSS (shown in Figure 9). It is assumed that the methods required to locate the MSS, determine angular rates, and Euler angles will be available to the shuttle crew. A stand-off position will be established approximately 200 ft from the MSS. MADD is then deployed. The detumble operation is broken down into three phases: (1) thrust-free orbital transfer to a rendezvous point, (2) thrusted pacing with the docking port and docking, and (3) detumbling of the MSS. MADD becomes automatic at the redezvous point and data is telemetered to the shuttle. Radio and visual contact may be lost intermittently because of occultation.

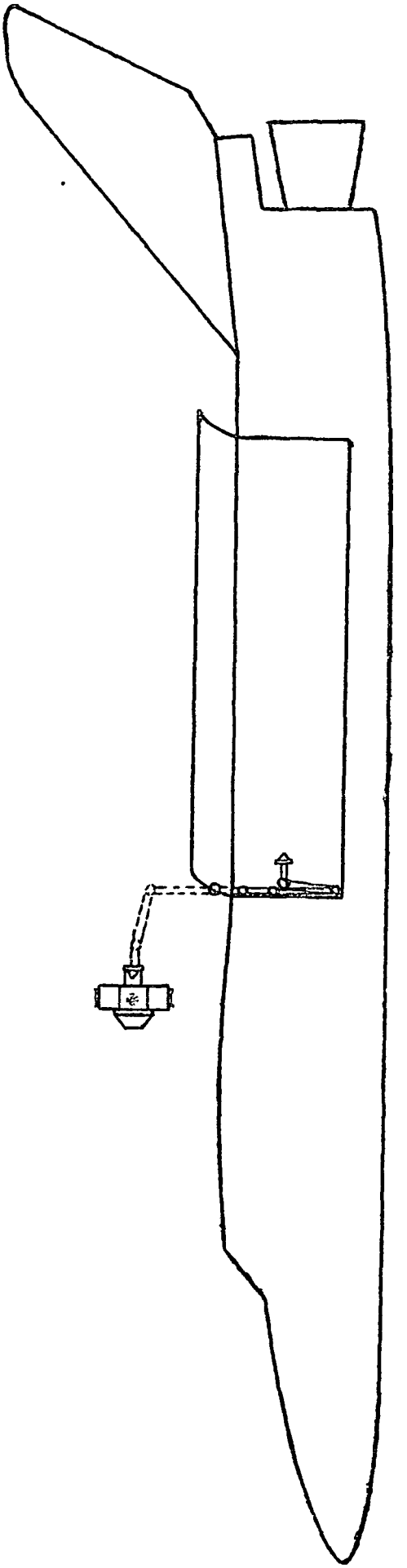

Figure 8 MADD Deployment Arrangement

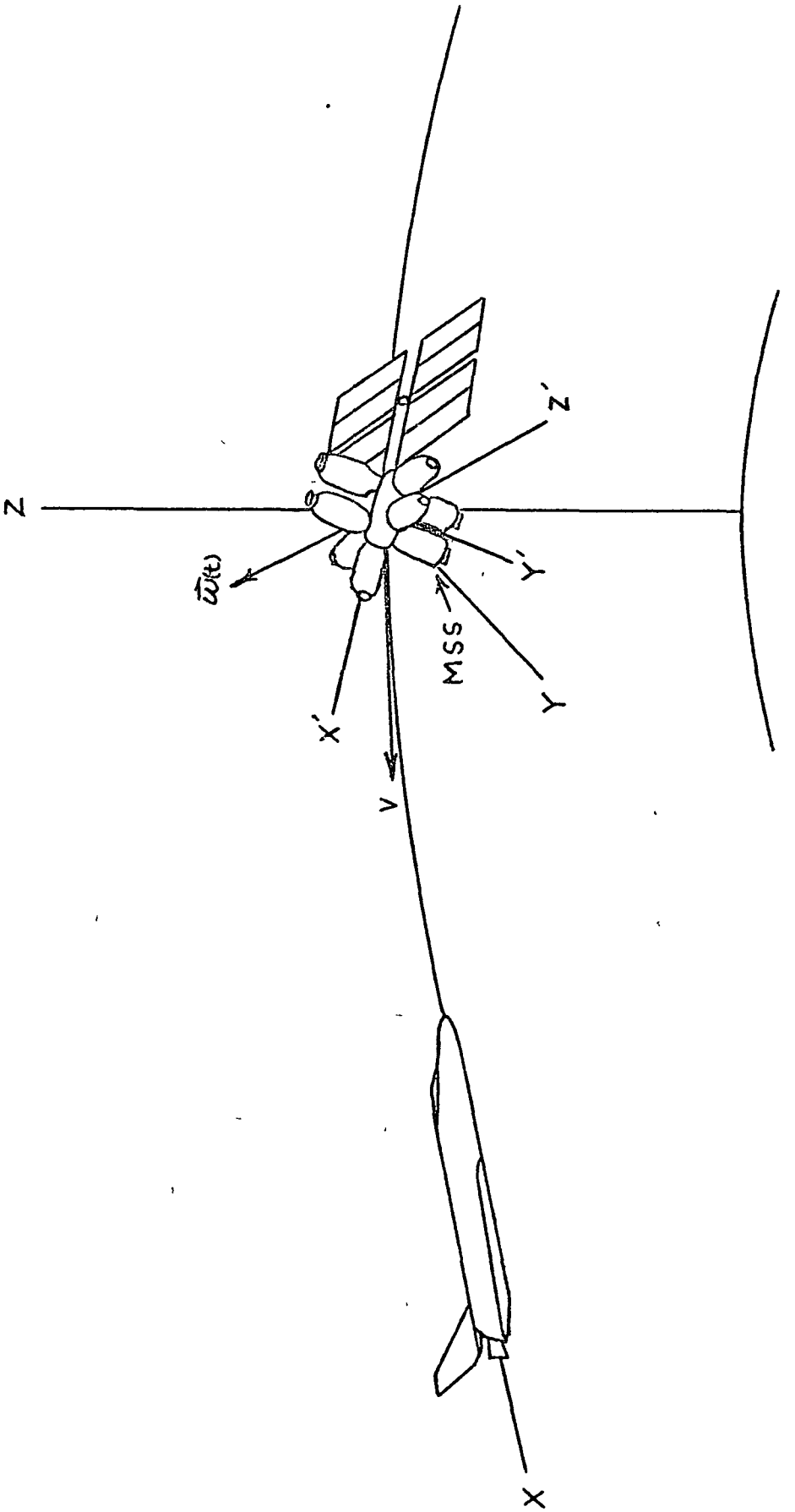

Figure 9 Shuttle/MSS Relative Position Nomenclature

The rendezvous point is chosen so that the velocity vector at the instant MADD reaches it, will coincide with zero velocity in the MSS moving coordinate frame. This would eliminate the need for a terminal maneuver to reorient the velocity vector and also reduce the risk of a collision with the MSS. Another constraint is that the trajectory must not allow MADD to collide with the MSS on its way to the rendezvous point. The actual transfer to the rendezvous point may require several impulses and corrections. An ideal transfer would require only one impulse.

At the rendezvous point MADD should be approximately 10 ft away from the docking port. Thrusters begin firing to keep pace with the docking port while closing into dock (shown in Figure 10). Passive docking aids will be required around the docking port for sensing relative position, orientation, and velocity. This permits proper alignment during closure and docking. MADD continues closure until the docking probe has engaged and capture latches are secured.

Once docked angular rates are measured, and a thrust profile is computed. Thrusters can then detumble quickly. Once angular rates reach zero, thrusting is stopped and evacuation of crewmen can take place.

IV. Transfer Trajectories

Transfer of MADD from shuttle to MSS is divided into two phases. Phase one is idealized as having one applied impulse chosen so that the vehicle has appropriate position and velocity

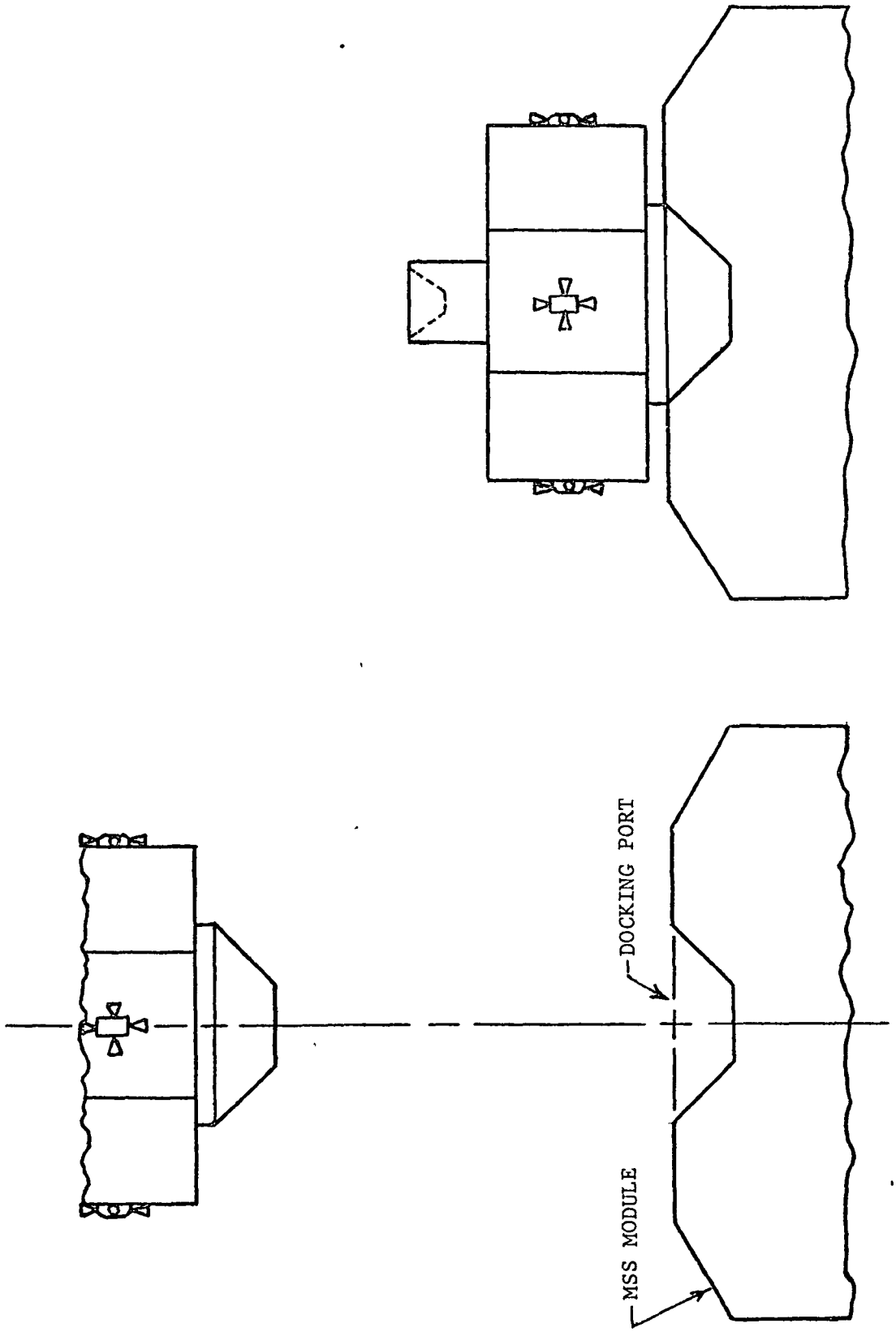

Figure 10 Rendezvous and Docking Configuration

components at the rendezvous point. During phase two MADD paces the docking port while closing into dock. Thrust computations are performed in a moving coordinate frame with the origin at the CG of the MSS as illustrated in Figure 9. The X-axis is along the direction of motion, Y-axis is normal to the orbital plane, and Z-axis is along the local vertical. Equations of motion for a transfer trajectory to an object in a nearly circular orbit are well-known.[3] In the moving X,Y,Z frame during phase one, these equations are

$$\left.\begin{aligned} &\ddot{x} + 2n\dot{z} = 0 \\ &\ddot{y} + n^2 y = 0 \\ &\ddot{z} - 2n\dot{x} - 3n^2 z = 0 \end{aligned}\right\} \qquad (1)$$

where $n = (GM_E/a^3)^{1/2}$, the mean motion of the MSS in its orbit. The solution of set (1) is readily obtained in closed form:

$$\left.\begin{aligned} x(t) &= \frac{2\dot{z}_o}{n}\cos nt + \left(\frac{4\dot{x}_o}{n} + 6z_o\right)\sin nt + \left(x_o - \frac{2\dot{z}_o}{n}\right) - (3\dot{x}_o + 6nz_o)t \\ y(t) &= y_o \cos nt + \frac{\dot{y}_o}{n}\sin nt \\ z(t) &= \frac{\dot{z}_o}{n}\sin nt - \left(\frac{2\dot{x}_o}{n} + 3z_o\right)\cos nt + \left(\frac{2\dot{x}_o}{n} + 4z_o\right) \end{aligned}\right\} \qquad (2)$$

With initial conditions

$$x(0) = x_o,\ y(0) = z(0) = 0$$

set (2) becomes

$$\left.\begin{aligned} x(t) &= \frac{2\dot{z}_o}{n}\cos nt + \frac{4\dot{x}_o}{n}\sin nt + \left(x_o - \frac{2\dot{z}_o}{n}\right) - 3\dot{x}_o t \\ y(t) &= \frac{\dot{y}_o}{n}\sin nt \\ z(t) &= \frac{\dot{z}_o}{n}\sin nt - \frac{2\dot{x}_o}{n}\cos nt + \frac{2\dot{x}_o}{n} \end{aligned}\right\} \qquad (3)$$

Initial conditions are based on the assumption that the shuttle is in the orbital plane of the MSS. The out-of-plane Y-component results in simple harmonic motion, while in-plane transfer motion is coupled. The only acceptable values of initial conditions x_o, $\dot{x}_o$, $\dot{y}_o$, and $\dot{z}_o$ are those which result in x, y, z and $\dot{x}$, $\dot{y}$, $\dot{z}$ simultaneously approaching the values x_1, y_1, z_1 and v_{1x}, v_{1y}, v_{1z}, respectively at time $t = t_1$, (rendezvous point). The initial velocity components are given as

$$\left.\begin{aligned} \dot{x}_o &= \frac{n(x_1 - x_o)\sin nt_1 + 2nz_1(1 - \cos nt_1)}{8(1 - \cos nt_1) - 3nt_1 \sin nt_1} \\ \dot{y}_o &= \frac{ny_1}{\sin nt_1} \\ \dot{z}_o &= \frac{nz_1(4 \sin nt_1 - 3nt_1) - 2n(x_1 - x_o)(1 - \cos nt_1)}{8(1 - \cos nt_1) - 3nt_1 \sin nt_1} \end{aligned}\right\} \quad (4)$$

These resulting expressions indicate that the initial relative velocity requirements for transfer to the rendezvous point are functions of x_o, x_1, y_1, z_1, and time of transfer, t_1. x_o is dependent upon safety of the shuttle to prevent a hazardous situation, and x_1, y_1, z_1 are dependent upon the location of the docking port at time $t = t_1$. The velocity components are given as

$$\left.\begin{aligned} \dot{x}(t) &= -2\dot{z}_o \sin nt + 4\dot{x}_o \cos nt - 3\dot{x}_o \\ \dot{y}(t) &= \dot{y}_o \cos nt \\ \dot{z}(t) &= \dot{z}_o \cos nt + 2\dot{x}_o \sin nt \end{aligned}\right\} \quad (5)$$

At time t_1 the velocity components of MADD should be equal to the velocity that point x_1, y_1, z_1 would have if it were fixed to the MSS. Therefore, the velocity components at time t_1 are[4]

$$\left.\begin{aligned} \dot{x}_1 &= \omega_y z_1 - \omega_z y_1 = -2\dot{z}_o \sin nt_1 + 4\dot{x}_o \cos nt_1 - 3\dot{x}_o \\ \dot{y}_1 &= \omega_z x_1 - \omega_x z_1 = \dot{y}_o \cos nt_1 \\ \dot{z}_1 &= \omega_x y_1 - \omega_y x_1 = \dot{z}_o \cos nt_1 + 2\dot{x}_o \sin nt_1 \end{aligned}\right\} \quad (6)$$

From these previous expressions, time t_1 and initial velocity requirements may be determined. ω_x, ω_y, ω_z, x_1, y_1, and z_1 are relative to the moving coordinate frame. They are related to the body fixed coordinate frame of the MSS by the following expressions.[4]

$$\begin{bmatrix} x_1 \\ y_1 \\ z_1 \end{bmatrix} = \underline{T(t_1)} \begin{bmatrix} x'_1 \\ y'_1 \\ z'_1 \end{bmatrix} \quad (7)$$

$$\begin{bmatrix} \omega_x \\ \omega_y \\ \omega_z \end{bmatrix} = \underline{T(t_1)} \begin{bmatrix} \omega'_x \\ \omega'_y \\ \omega'_z \end{bmatrix} \quad (8)$$

where

$$\underline{T(t_1)} = \begin{bmatrix} C\phi\, C\psi - S\phi\, S\psi\, C\theta & -S\phi\, C\psi - C\phi\, S\psi\, C\theta & S\theta\, S\psi \\ C\phi\, S\psi - S\phi\, C\psi\, C\theta & -S\phi\, S\psi + C\phi\, C\psi\, C\theta & -S\theta\, C\psi \\ S\theta\, S\phi & S\theta\, C\phi & C\theta \end{bmatrix} \quad (9)$$

using $C\phi = \cos\phi$, $S\phi = \sin\phi$, etc.

Automatic position control during phase two can be modeled by using the non-homogeneous form of equations (1)

$$\left.\begin{aligned} \ddot{x} + 2n\dot{z} &= f_x \\ \ddot{y} + n^2 y &= f_y \\ \ddot{z} - 2n\dot{x} - 3n^2 z &= f_z \end{aligned}\right\} \qquad (10)$$

where f_x, f_y, f_z are the applied acceleration components which are the control forces. Initial conditions associated with set (10) become

$$x(0) = x_1,\ y(0) = y_1,\ z(0) = z_1$$

$$\dot{x}(0) = \dot{x}_1,\ \dot{y}(0) = \dot{y}_1,\ \dot{z}(0) = \dot{z}_1$$

Taking the Laplace transform of the differential equations and solving for X(S), Y(S), and Z(S) gives

$$\left.\begin{aligned} X(S) &= \frac{1}{S}x_1 - \frac{6n^3}{S^2(S^2+n^2)}z_1 + \frac{S^2-3n^2}{S^2(S^2+n^2)}\dot{x}_1 - \frac{2n}{S(S^2+n^2)}\dot{z}_1 \\ &\quad + \frac{S^2-3n^2}{S^2(S^2+n^2)}F_x(S) - \frac{2n}{S(S^2+n^2)}F_z(S) \\ Y(S) &= \frac{Sy_1+\dot{y}_1}{S^2+n^2} + \frac{1}{S^2+n^2}F_y(S) \\ Z(S) &= \frac{1}{S^2+n^2}\dot{z}_1 + \frac{S^2+4n^2}{S(S^2+n^2)}z_1 + \frac{2n}{S(S^2+n^2)}\dot{x}_1 \\ &\quad + \frac{1}{S^2+n^2}F_z(S) + \frac{2n}{S(S^2+n^2)}F_x(S) \end{aligned}\right\} \qquad (11)$$

An example transfer trajectory is shown in Figure 11.

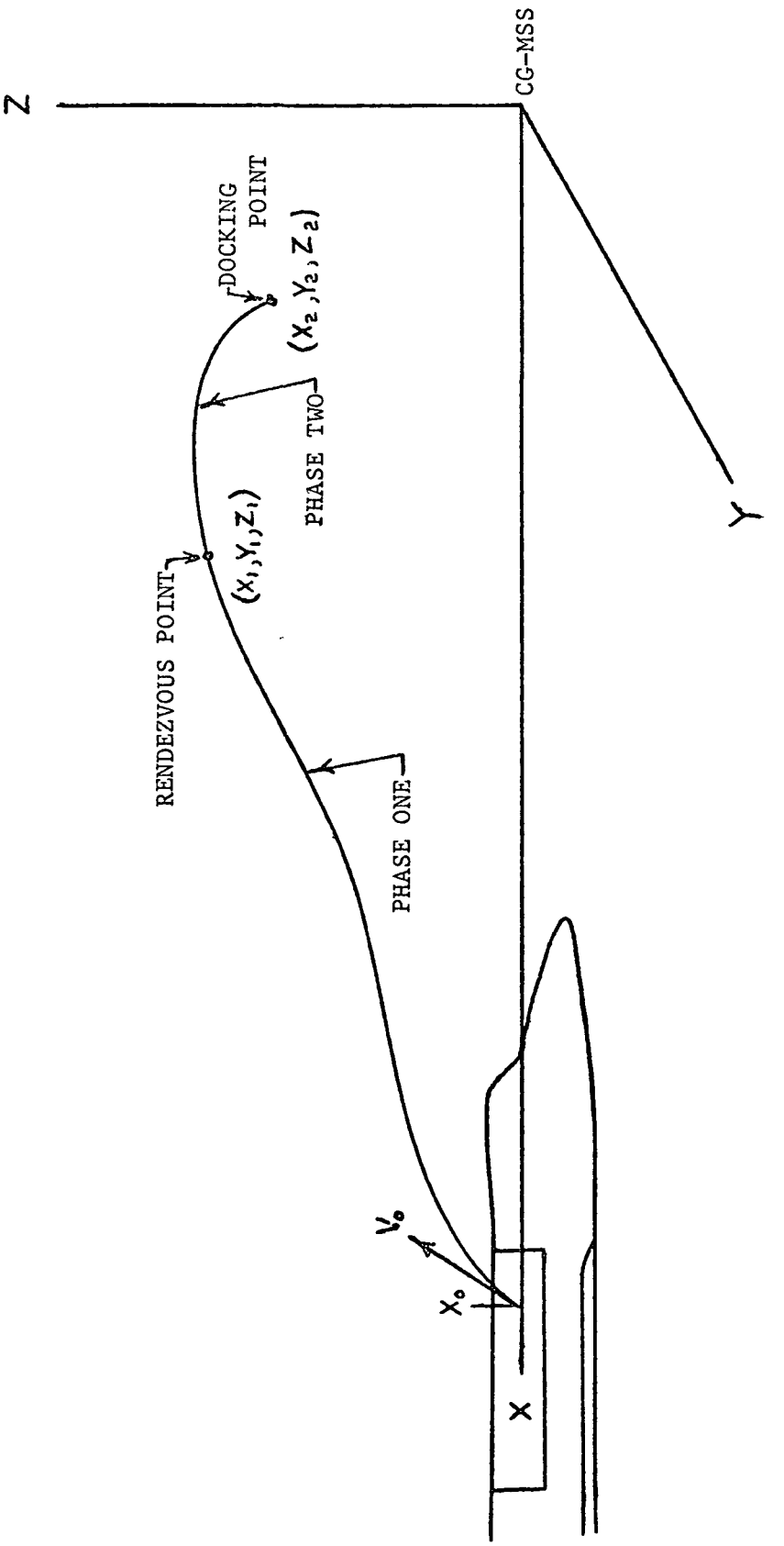

Figure 11 Typical Transfer Trajectory of MADD

V. Attitude Control Systems

Development of the attitude control systems for MADD is considered in this section. Two attitude control systems are required during the mission: (1) momentum exchange during phase one, and (2) mass expulsion during phase two and three. During phase one twin gyro controllers are used. Their advantages include: (1) first order cross-coupling terms are eliminated by using two-counter-rotating gyros, (2) less power and weight are required for a given momentum exchange capability, and (3) larger gimbal angles may be used so that a major portion of the stored momentum can be transferred to MADD. The equations of motion for a twin gyro controller are[5]

$$\left.\begin{aligned} I_x\dot{p} &= -2C_z\Omega_z\dot{\delta}_z + L_x \\ I_y\dot{q} &= -2C_x\Omega_x\dot{\delta}_x + L_y \\ I_z\dot{r} &= -2C_y\Omega_y\dot{\delta}_y + L_z \end{aligned}\right\} \qquad (12)$$

The small perturbation approach was used to uncouple the equations, thus, the second-order terms can be neglected. From the equations, it is apparent that the controller on the X-axis controls the Y-axis, Y controls Z, and Z controls X, respectively. By using identical gyros on all three axes.

$$C = C_x = C_y = C_z \text{ and } \Omega = \Omega_x = \Omega_y = \Omega_z$$

Therefore, the control equations for each axis are the same except for the moment of inertia about that axis. The three axes can be controlled by an identical control system except for the system gain which would vary with the moments of inertia.

Orientation of MADD during phase two is accomplished by placing thrusters about the control axes. Mass-expulsion devices are inefficient as compared to momentum-exchage devices. Thrusters were chosen because the spin vector is not inertially oriented, and momentum-exchange devices are incapable of continuously reorienting the spin vector without continuous momentum dumping.

Geometry of the coordinate frames relative to the moving frame are shown in Figure 12. The coordinate frame of MADD is translated in the Z direction and the X and Y axes remain parallel to those of the docking reference. The docking reference frame is translated relative to the body fixed axes of the MSS and is fixed. With these conditions, proper orientation of MADD will occur when Euler angles and rates are equal to those of the body fixed frame relative to the moving coordinate frame. Therefore, angular rates about the respective axes should be equal. Assuming that the orbital angular velocity is small compared with the tumbling angular velocity, motion of MADD with applied torques is given by[4]

$$\left.\begin{aligned} I_x\dot{p} + qr(I_z - I_y) &= m_x \\ I_y\dot{q} + pr(I_x - I_z) &= m_y \\ I_z\dot{r} + pq(I_y - I_x) &= m_z \end{aligned}\right\} \quad (13)$$

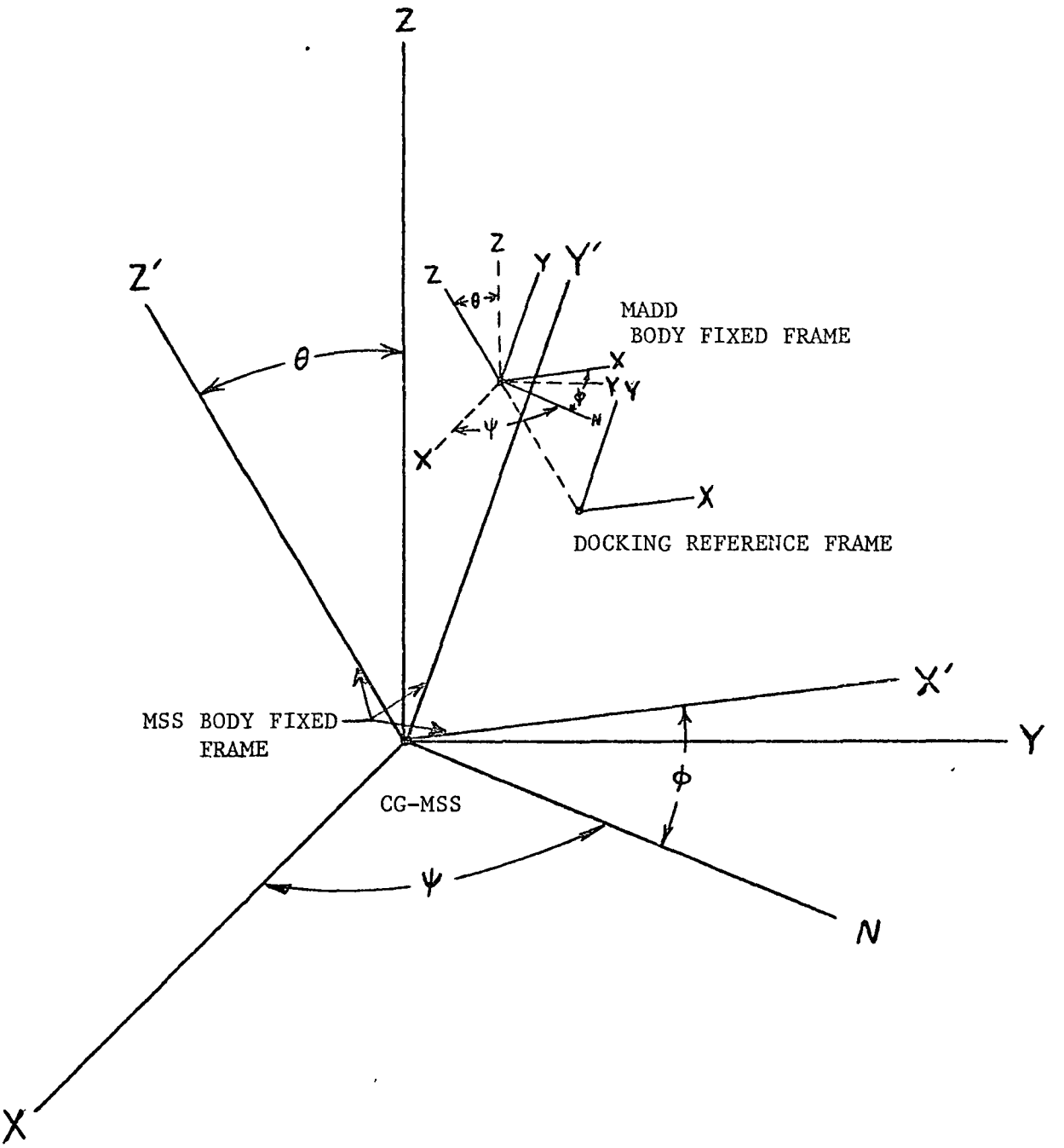

Figure 12 MADD/MSS Relative Position Nomenclature

m_x, m_y, m_z are applied torques, including both disturbance and control moments. Initial conditions associated with set (13) are

$$p(0) = p_o,\ q(0) = q_o,\ r(0) = r_o$$

Taking the Laplace transform of the differential equations and solving for P(S), Q(S), R(S) gives

$$\left.\begin{aligned} P(S) &= \frac{1}{S} p_o + \frac{1}{S} M_x(S) - \frac{Q(S)\,R(S)}{S}\left(\frac{I_z - I_y}{I_x}\right) \\ Q(S) &= \frac{1}{S} q_o + \frac{1}{S} M_y(S) - \frac{P(S)\,R(S)}{S}\left(\frac{I_x - I_z}{I_y}\right) \\ R(S) &= \frac{1}{S} r_o + \frac{1}{S} M_z(S) - \frac{P(S)\,Q(S)}{S}\left(\frac{I_y - I_x}{I_z}\right) \end{aligned}\right\} \quad (14)$$

Control laws and stability criterion must be developed next. This will be part of the continuing development of the MADD concept.

VI. Conclusions

Problems related to docking with and detumbling a passive modular space station have been considered here. A MADD concept is proposed as a means to apply torques to detumble the MSS, and a preliminary design is presented. An operational procedure has been outlined and subsystems discussed. Appropriate assumptions on mission requirements and constraints were formulated based on expected future programs and developments. Position and attitude control systems are being developed which will permit completely automatic dock and detumble.

VII. References for Appendix C

1. Snow, W. R., "Analysis of Worst Case Tumbling Motions of Selected Space Vehicles," Appendix A, Semi-Annual Progress Report on Dynamics and Control of Escape and Rescue from a Tumbling Spacecraft, NASA Grant 39-009-210, December 1971, pp. 7-50.

2. Kendrick, J. B., "TRW Space Data," TRW Systems Group, TRW Inc., 1967, pp.67.

3. Eggleston, J. M. and Beck, H. D., "A Study of the Position and Velocities of a Space Station and Ferry Vehicle During Rendezvous and Return," NASA TR R-87, 1961.

4. Thompson, W. T., Introduction to Space Dynamics, John Wiley and Sons, Inc., New York, 1963, pp. 22, 33-38, 113.

5. Greensite, A. L., "Attitude Control in Space," Analysis and Design of Space Vehicle Flight Control Systems, Vol. XII, NASA CR-831, Washington, D.C., August 1967, pp. 13-23, 40-55.

APPENDIX D

Optimal Detumbling Analyses

(B. Kunciw)

I. Discussion

The minimum time optimal detumbling of a distressed space vehicle can be divided into the following categories: constraint on magnitude of control moment vector and constraint on magnitude of each component of this vector. In the first NASA Rescue Progress Report the problem of detumbling a distressed space vehicle in minimum time was identified, i.e., bring the angular velocities to zero. The space vehicle is modeled as a rigid body by Euler's moment equations:[1]

$$m_x = A\dot{\omega}_x + \omega_y\omega_z\,(C-B)$$

$$m_y = B\dot{\omega}_y + \omega_x\omega_z\,(A-C)$$

$$m_z = C\dot{\omega}_z + \omega_x\omega_y\,(B-A).$$

Singularity difficulties were encountered when optimal equations were being determined. This was due to the linearity of Euler's equations in the control moments m_1. Thus, upon applying

$$\frac{\partial H}{\partial u} = 0$$

where H = Hamiltonian

and u = control moment

For the determination of the optimal control moment, it was observed that the control moment was being differentiated out of the optimization equations.[2] Subsequent investigation showed that the above difficulty could be avoided if constraints were placed on the control moments. As stated previously, the two types of constraints are:

$$(u_1^2 + u_2^2 + u_3^2)^{1/2} \leq M$$

$$|u_k| \leq m_k \qquad k = 1,2,3.$$

The first type of constraint leads to a fairly simple solution.[3] It turns out that the required orientation of the control moment is opposite to the angular momentum vector and its magnitude is the largest available from the reaction jets. Writing

$$x_k = I_k \omega_k \qquad k = 1,2,3$$

where I_k = moment of inertia about k axis and placing into Euler's moment equations we get

$$\dot{x}_1(t) = \alpha_1 x_2(t)\, x_3(t) + u_1(t)$$

$$\dot{x}_2(t) = \alpha_2 x_3(t)\, x_1(t) + u_2(t)$$

$$\dot{x}_3(t) = \alpha_3 x_1(t)\, x_2(t) + u_3(t)$$

where

$$\alpha_1 = \frac{I_2 - I_3}{I_2 I_3}$$

$$\alpha_2 = \frac{I_3 - I_1}{I_3 I_1}$$

$$\alpha_3 = \frac{I_1 - I_2}{I_2 I_1} \quad .$$

The optimal control moment is

$$u_{\text{min time}}(t) = -m \frac{\vec{\hat{x}}^*(t)}{||\vec{\hat{x}}^*(t)||}$$

where

$$||\vec{\hat{x}}^*(t)|| = [x^*_1{}^2(t) + x^*_2{}^2(t) + x^*_3{}^2(t)]^{1/2}$$

and

$\vec{\hat{x}}^*(t)$ is the solution of

$$\dot{\vec{\hat{x}}}(t) = \vec{\hat{f}}[\vec{\hat{x}}(t);t] - m \frac{\vec{\hat{x}}(t)}{||\vec{\hat{x}}(t)||}$$

starting from $x_i(t_o) = \zeta_i$, $i = 1,2,3$ to origin ($x_i = 0$, $i = 1,2,3$).

For our case we get, for $\dot{\vec{\hat{x}}}(t)$:

$$\dot{x}_1(t) = \alpha_1 x_2(t) x_3(t) - \frac{m x_1(t)}{[x_1{}^2(t) + x_2{}^2(t) + x_3{}^2(t)]^{1/2}}$$

$$\dot{x}_2(t) = \alpha_2 x_3(t)\ x_1(t) - \frac{m\ x_2(t)}{[x_1^2(t) + x_2^2(t) + x_3^2(t)]^{1/2}}$$

$$\dot{x}_3(t) = \alpha_3 x_1(t)\ x_2(t) - \frac{m\ x_3(t)}{[x_1^2(t) + x_2^2(t) + x_3^2(t)]^{1/2}}$$

These equations were applied to the tumbling MSS caused by collision with the Mark II Orbiter assuming 100% kinetic energy exchange.[4] The principal axis angular velocities at commencement of thrusting were chosen at t = 120 sec. after collision; here the ω_i's are fairly large so as to give a good test to this optimization technique. The angular velocities are 1.150, 1.750 and -0.445 RPM's about 1, 2 and 3 principal axes, respectively. These velocities were brought to near zero in about 7 minutes with the application of a maximum control moment vector magnitude (m) of 2500 ft-lbs. Figure 13 shows a time history of the principal axis angular velocities during application of the optimum control moment. Figure 14 gives a time history of the body fixed thrusts (lbs.) required at point x = 12.8', y = 2.9' and z = 60.0' to give the necessary 2500 ft-lb moment directed opposite to the angular momentum vector.

The second type of constraint ($u_i \leq m_i$, i = 1,2,3) presents more difficulty in determining the optimum minimum time control moment sequence. In this case, the analysis is not as easily accomplished; the control moment vector is not simply directed

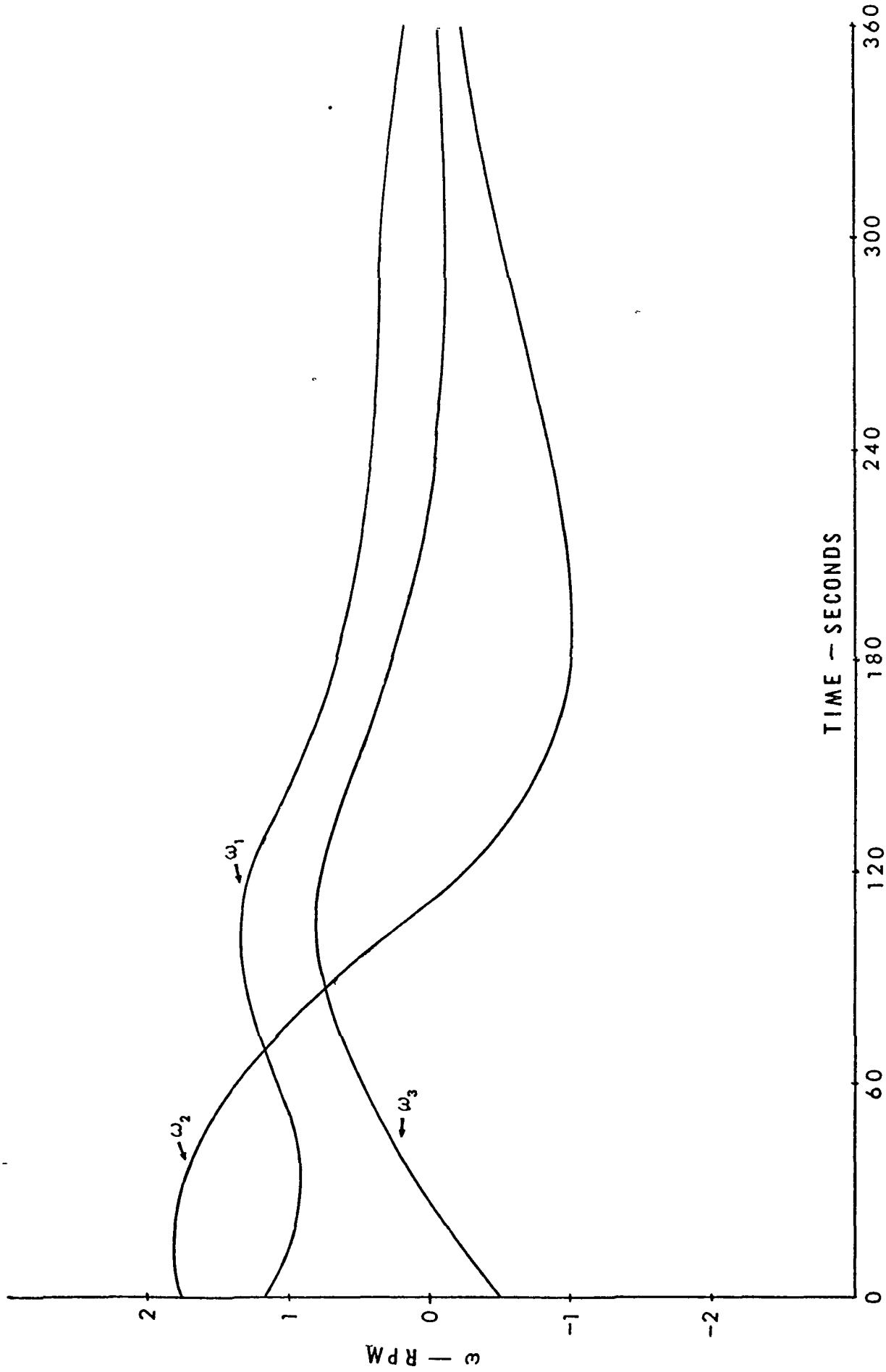

Figure 13. Principal Angular Velocities During Detumbling

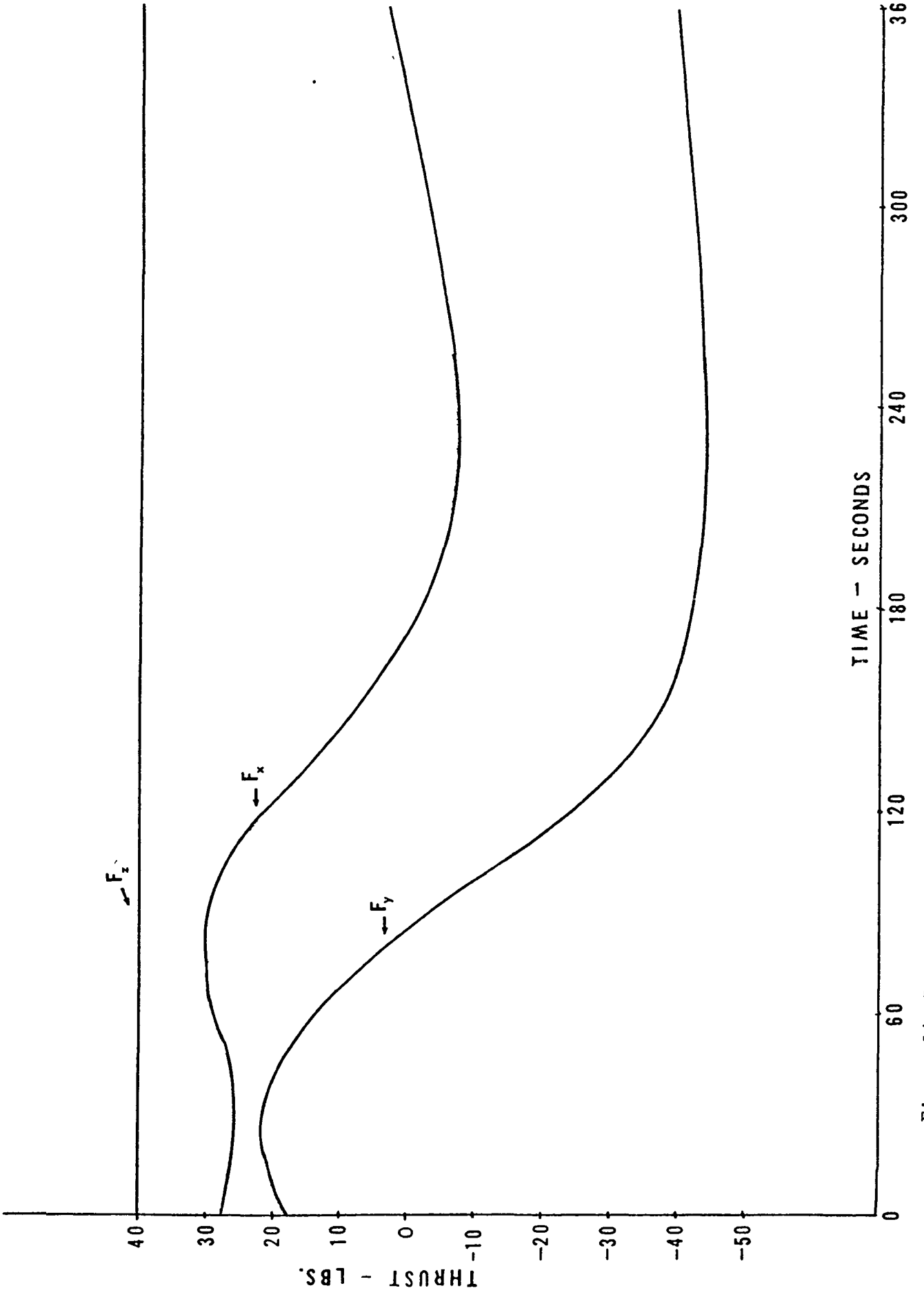

Figure 14. Body Fixed Thrust at X = 12.8' Y = 2.9' Z =-60.0' for 2500 ft-lbs Max. Torque

opposite to the angular momentum vector. As subsequent analysis will show, the magnitudes of the components (u_i) of the control moment vector ($\vec{u}$) will be the largest possible (m_i) - what will change will be the direction of thrust (+, -). This change in directions of thrust (switching times) is, in fact, of major concern in this type of analysis. The equations describing minimum time detumbling for the constraint $u_i \leq m_i$ are as follows:

$$\dot{x}_1(t) = \alpha_1 x_2(t)\ x_3(t) + u_1(t)$$

$$\dot{x}_2(t) = \alpha_2 x_3(t)\ x_1(t) + u_2(t)$$

$$\dot{x}_3(t) = \alpha_3 x_1(t)\ x_2(t) + u_3(t)$$

where

$$x_k(t) = I_k \omega_k(t)$$

$\omega_k(t)$ = angular velocity about k^{th} axis

I_k = moment of inertia about k^{th} axis,

$$H = 1 + p_1(t)\ \dot{x}_1(t) + p_2(t)\ \dot{x}_2(t) + p_3(t)\ \dot{x}_3(t)$$

$$= 1 + p_1(t)\ \alpha_1 x_2(t)\ x_3(t) + p_1(t)\ u_1(t)$$

$$+ p_2(t)\ \alpha_2 x_3(t)\ x_1(t) + p_2(t)\ u_2(t)$$

$$+ p_3(t)\ \alpha_3 x_1(t)\ x_2(t) + p_3(t)\ u_3(t),$$

$$\dot{p}_k(t) = -\frac{\partial H}{\partial x_k}$$

which yields

$$\dot{p}_1(t) = -\alpha_2 x_3(t)\ p_2(t) - \alpha_3 x_2(t)\ p_3(t)$$

$$\dot{p}_2(t) = -\alpha_1 x_3(t)\ p_1(t) - \alpha_3 x_1(t)\ p_3(t)$$

$$\dot{p}_3(t) = -\alpha_1 x_2(t)\ p_1(t) - \alpha_2 x_1(t)\ p_2(t)$$

and

$$u_i(t) = u_{i_{\text{min time}}} = -\, m_i \operatorname{sgn}\ \{p_i(t)\}$$

which gives

$$u_1(t) = -\, m_1 \operatorname{sgn}\ \{p_1(t)\}$$

$$u_2(t) = -\, m_2 \operatorname{sgn}\ \{p_2(t)\}$$

$$u_3(t) = -\, m_3 \operatorname{sgn}\ \{p_3(t)\}\ .$$

As can be seen from the above equations for the control moment components $u_1(t)$, $u_2(t)$ and $u_3(t)$, the control history will be of a bang-bang type; this requires investigation for the switching times. This investigation will be made in conjunction with techniques to solve the system of optimization equations. Linear programming will be given priority over the methods of steepest descent and successive sweep or a combination of the two methods. The reason for this choice is the sensitivity of successive sweep to the

initial guess for the control history, and the many iterations frequently required and the frequent non-convergence to the time minimum of steepest descent; a combination of steepest descent and successive sweep unnecessarily complicates and lengthens the analysis and computation when compared to linear programming. Linear programming is relatively insensitive to the normal control history and converges quickly; also, it uses linear programs for digital computers presently available.

II. Conclusions

Research to date shows that detumbling of the MSS can be accomplished in a few minutes with very small reaction jets. Furthermore, it can be stated that structural limitations of the MSS and human tolerance are not exceeded by the induced "g" loads, and that the fuel weight is low. Investigation into the constraint $|u_i| \leq m_i$, where i = 1, 2, 3 will permit the choosing of the best possible configuration of reaction jets on a rescue module and the best detumbling control sequence.

III. References for Appendix D

1. Thomson, William Tyrell, Introduction to Space Dynamics, John Wiley and Sons, Inc., New York, 1961.

2. Bryson, Arthur E., Jr., and Ho. Yu-Chi, Applied Optimal Control, Ginn and Company, Massachusetts, 1969.

3. Athans, Michael and Falb, Peter L., Optimal Control, MsGraw-Hill, Inc., New York, 1966.

4. 1st NASA Rescue Report, Dr. M. Kaplan, Principal Investigator, The Pennsylvania State University, December 1971.

APPENDIX E

Flexibility Effects on Free Motion

(J. Stimpson)

I. Introduction

Many methods have been employed to study the motion of nonrigid spacecraft. Classical approaches, such as discrete coordinate and normal mode formulations, have been used in the past with relative success when applied to relatively simple spacecraft configurations. Most modern spacecraft have large nonrigid parts; and the effect these flexible parts will have on the motion of modern space vehicles are under study. Therefore, an extensive review of techniques used in dealing with flexibility has been made, and this report will briefly describe some of the flexibility modelling techniques available today.

II. Survey of Techniques

In reviewing the "state of the art" concerning mathematical formulation of nonrigid spacecraft, it has been found that each method will fall into one of three categories: (1) discrete coordinate formulation; (2) vehicle normal-mode coordinate formulation; and (3) hybrid-coordinate formulation.

If one can model a spacecraft as a collection of interconnected rigid bodies then the discrete coordinate formulation is applied. One discrete coordinate method, known as the augmented body approach, considers a spacecraft modelled as an n-body, point-connected collection of rigid bodies assembled in a topological tree (no closed loops). Now an augmented body consists

of the ith body of the set together with certain particles (point masses) attached to each of the joints of that body. An example of an augmented body is given in Figure 15.

The mass center of the augmented body is called the connection barycenter (or simply the barycenter). Now the form of the dynamical equations for the attitude motion of a set of bodies as described by this method[1] is:

$$\underline{\underline{\phi}}_\lambda^* \cdot \underline{\omega}_\lambda + \underline{\omega}_\lambda \times \underline{\underline{\phi}}^* \cdot \underline{\omega}_\lambda = \underline{T}_\lambda + \sum_{j \in J_\lambda} \underline{T}''_{\lambda j} + \underline{D}_\lambda \times \underline{F}_\lambda + \tag{1}$$

$$\sum_{\mu \neq \lambda} \underline{D}_{\lambda\mu} \times \underline{F}_\mu + M \sum_{\mu \neq \lambda} \underline{D}_{\lambda\mu} \times [\dot{\underline{\omega}}_\mu \times \underline{D}_{\mu\lambda} + \underline{\omega}_\mu \times (\underline{\omega}_\mu \times \underline{D}_{\mu\lambda})]$$

where

$\underline{\underline{\phi}}_\lambda^*$ = the inertia dyadic of the λth augmented body, referred to the corresponding barycenter

$\underline{\omega}_\lambda$ and $\underline{\omega}_\mu$ = the inertial angular velocities of bodies λ and μ, respectively

$\underline{T}_\lambda$ = that portion of the resultant torque applied to body obtained by excluding forces and torques applied at joints

$\underline{T}_{\lambda_j}^H$ = the "hinge torque" applied at point j of body

J_λ = the set of numeric labels for the joints on body λ

$\underline{D}_\lambda$ = the position vector from the barycenter B_λ to the mass center of body

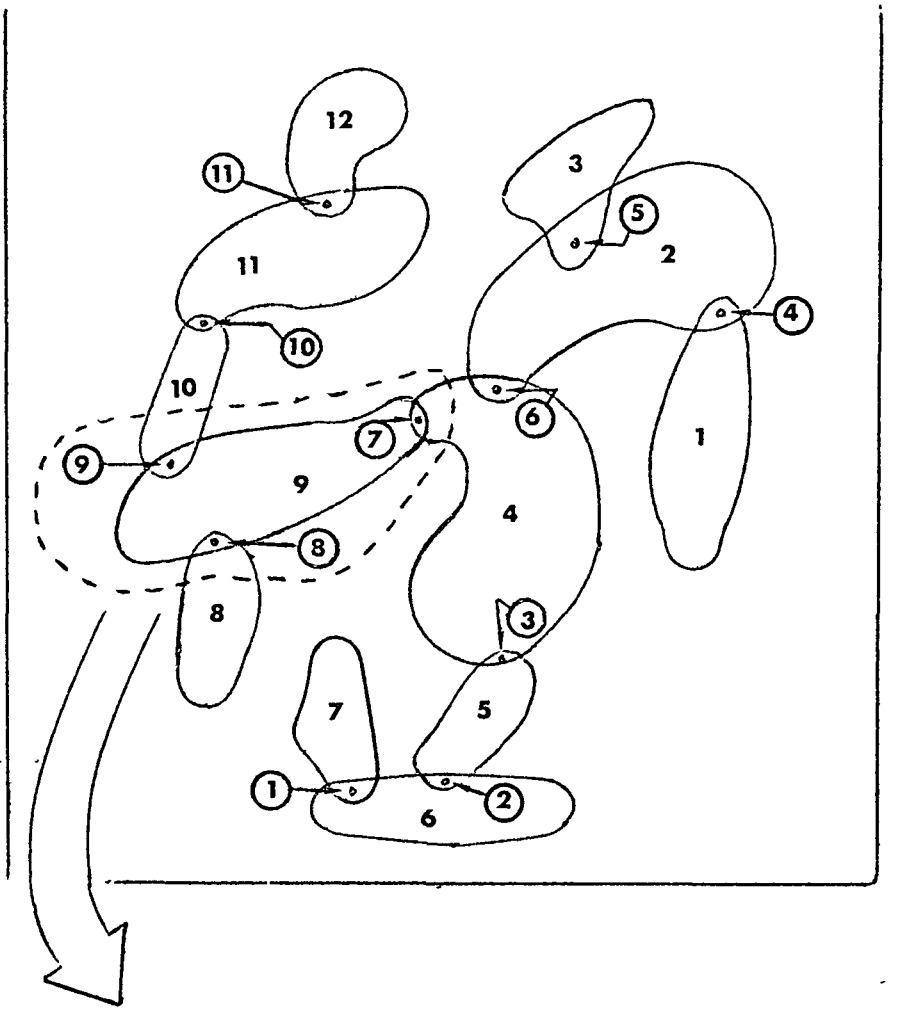

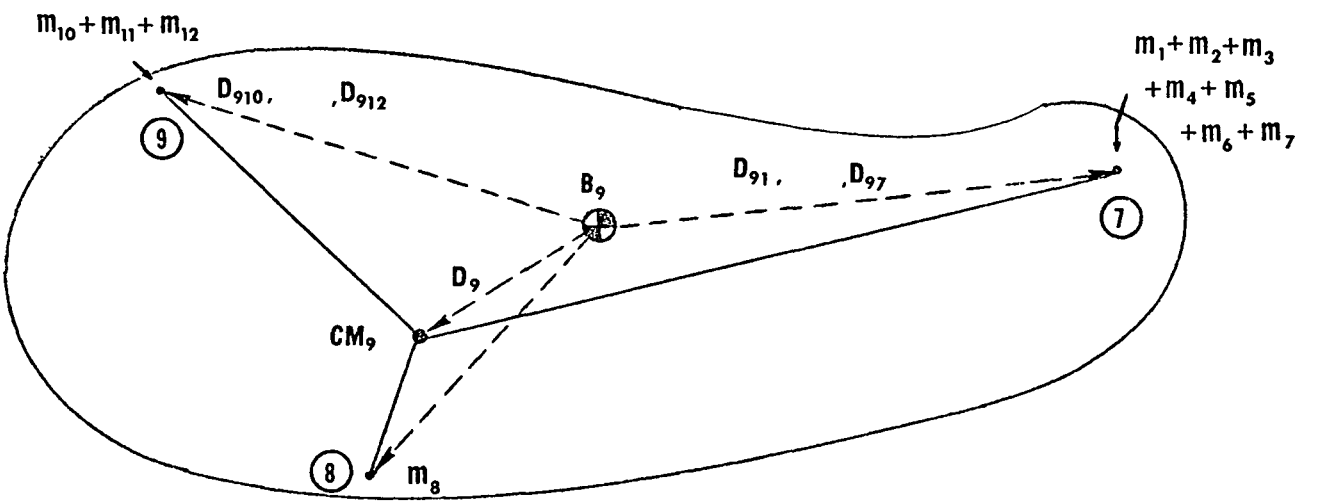

Figure 15. Augmented Body 9 and it Barycenter B_9

$\underline{F}_\lambda$ and $\underline{F}_\mu$ = the forces applied to bodies λ and μ respectively, excluding forces applied at joints.

$\underline{D}_{\lambda\mu}$ = the position vector from the barycenter B_λ the joint of body λ that leads to body μ (even if body is not directly connected to body λ, but instead is part of a chain of bodies connected to body λ.

M = the total system mass

$\sum_{j \in J_\lambda}$ = sum over values of j in the set J_λ

The overdots denote time derivatives in an inertial reference frame.

In general, there are n-vector-dyadic equations like equation 1 to complete a dynamical description of the system as well as some specifications on the hinge torques $T^H_{\lambda_j}$. Suppose the augmented body b_λ has a connection at point j which does not permit three degrees of rotational freedom. Then absolute constraints must be imposed on the relative motion of the two bodies sharing point j; this would be the case if the connection at j were a hinge line, permitting only a simple planar relative rotation of the two bodies. Those components of $T^H_{\lambda j}$ which enforce the absolute constraints are unknown and generally unwanted constraint torques.[2] Hooker describes a way which can be implemented to eliminate the constraint torques.[3]

In another method utilizing the same topological tree configuration for the set of rigid bodies making up the spacecraft model, is the nested-body technique.[4] In this approach, one

writes the vector equations of motion in turn for n different subsets of bodies, including a final set of rotational and translational equations for the composite vehicle. The idea of isolating in sequence such subsets of rigid bodies in an n-body system seems to have both advantages and disadvantages. One disadvantage of this method lies in the difficulty of physical interpretation whereas the augmented body method utilizes such concepts as connection barycenter to help in the interpretation of the terms involved in the equations of motion. However, the nested body technique facilitates the elimination of internal constraint forces and torques.

Another method under the category of discrete coordinate formulation is concerned with generalized forces which implies Lagrangian formulation. This means that the Lagrange's equations:

$$\frac{d}{dt}\left(\frac{\partial L}{\partial \dot{q}_i}\right) - \frac{\partial L}{\partial q_i} = Q_i \quad i = 1, \ldots, n \tag{2}$$

where $q_1,..,q_n$ are a complete and independent set of generalized coordinates; L (the Lagrangian) is the difference in kinetic and potential energy and the generalized force Q_i is defined in terms of applied forces $F^1,...F^s$ and their inertial position vectors r^1, $...r^s$ by:

$$Q_i = \sum_{j=1}^{s} F^j \cdot \frac{\partial r^j}{\partial q_i} \qquad i = 1, \ldots, n \tag{3}$$

is employed.

The problem with the Lagrangian approach is that the method is restricted to only certain non-holonomic systems and the method has not yet led to a multi-purpose computer program for machine computation of the response of arbitrary discrete parameter systems.[4]

Now the methods utilizing the collection of rigid bodies in a topological true configuration is limited for simulating spacecraft motion. The largest n-body equation numerical integration programs now operative for unrestricted angular motions permit the simulation of dynamical systems with about thirty-degrees of freedom. Many spacecraft under development today simply cannot be modeled adequately as a collection of rigid bodies with less than one hundred degrees of freedom.

On the other hand, it is never necessary to permit large relative motions between all portions of a spacecraft portrayed as a system with hundreds of degrees of freedom. In other words, it is possible to partially linearize the system by restricting some of the coordinates to experience only small changes in magnitude. From structural dynamics, it is a well-established tradition to idealize a structure as linearly elastic and subject to small deformations so as to obtain linearized differential equations. It is further customary to characterize the structure as having a large but finite number of degrees of freedom, this practice involves subdividing the structure into a grid system whose intersection points are called nodes, and then defining the system behavior in terms of translations and rotations at the nodes.

The mass of the structure may be concentrated as particles at the nodes, or it may be distributed throughout the finite elements which interconnect the nodes.

This brings us to category two - the vehicle normal-mode coordinate method. This method consists of formulating equations of motion, whenever possible, as a systems of independent (uncoupled) scalar second-order differential equations. For certain physical systems, some transformation may be found to transform from some arbitrary selected coordinate system to a system corresponding to uncoupled scalar equations of motion. In general, each coordinate (called normal coordinates) is associated with a motion in which the entire vehicle participates. Because the equations of motion are uncoupled, the vehicle can oscillate at some natural frequency (normal-node frequency) and undergo a periodic deformation into some deformed shape (normal-mode shape) corresponding to the natural frequency. Now for any equation of motion of the class: $M'\ddot{q} + D'q + K'q = L'$ (4) where M' and K' are symmetric matrices and $D' = \alpha M' + \xi K'$ with α and ξ arbitrary scalars, permits the normal-mode transformation, namely $q = \phi\eta$ where ϕ is a square matrix whose columns are the eigenvectors associated with equation 4. With this transformation and a premultiplication by ϕ^T, equation 4 becomes:

$$\ddot{\eta} + 2\xi\sigma\dot{\eta} + \sigma^2\eta = \phi^T L' \tag{5}$$

where ξ and σ are diagonal matrices containing, respectively, the percentages of critical damping and the natural frequencies of the modal coordinates η .

This classical approach to vibration analysis has not been widely used as a means to describe the motion of a nonrigid spacecraft due to its limitations. Application of this method to a system which includes nonlinearities, rotors, discrete dampers, or articulated moving parts cannot be done. Formulating the equations of motion as first-order (state) equations eliminates some of these obstacles. A first order form of Eqn. 5 is:

$$B\dot{Q} + CQ = F \tag{6}$$

where:

$$Q \equiv \begin{bmatrix} q^T \\ \hline \dot{q}^T \end{bmatrix} \quad , \qquad F \equiv \begin{bmatrix} 0 \\ \hline L^T \end{bmatrix}$$

and

$$B \equiv \left[\begin{array}{c|c} K & 0 \\ \hline 0 & M \end{array}\right] \quad , \qquad C \equiv \left[\begin{array}{c|c} 0 & -K \\ \hline K & D \end{array}\right]$$

and by applying a transformation to modal coordinates, $Q = \phi Y$ one will finally obtain the equation:

$$\dot{\bar{Y}} + \bar{\Lambda}\bar{Y} = (\phi'^T B \phi)^{-1} \phi'^T F \tag{7}$$

where

$\bar{Y}$ is $2N \times 1$ matrix of variables significant to the vehicle response.

$\bar{\Lambda}$ truncated version of the diagonal matrix of eigenvalues.

ϕ is the truncated version of the matrix of eigenvectors of Eqn. 6.

ϕ' is the corresponding truncated version of the matrix of eigenvectors of the homogeneous adjoint equation:

$$B^T\dot{Q}' + C^T Q' = 0$$

Equation 7 must be augmented with at least the equation $T = \dot{H}$ to describe the spacecraft motion. The difficulty with Equation 7 is that it is restricted to linearly elastic spacecraft undergoing small deformations which eliminates many spacecraft configurations. For example, the introduction of an actively controlled rotor along the pitch axis of a gravity-stabilized vehicle, or the introduction of an actively controlled despun platform to a spin-stabilized satellite violates the assumption leading to equation 7.

The vehicle normal mode methods have chiefly applied to the simulation of motion of missiles and launch vehicles and to the determination of passive linear response of a spacecraft structure to its dynamic environment during launch.

Now many variations of the techniques described as either a discrete coordinate or a vehicle normal-mode coordinate formulation have not been mentioned due to the great number of variations that exist. Most good structural dynamics books contain many of the classical approaches to flexibility not described in this report.[5]

The newest formulation in the area of flexibility analysis techniques is the hybrid coordinate formulation. Stimulated by the development of the larger and more complex modern spacecraft, the hybrid coordinate formulation attempts to perserve the generality

of the discrete coordinate formulation wherever necessary and secure the computational efficiency of the distributed coordinate formulation wherever possible.

This hybrid coordinate formulation is still being studied but the basic idea of the hybrid coordinate approach is to separate the spacecraft into a number of substructures, some being idealized as elastic and others as rigid, but with large relative motions permitted between interconnected substructure. The flexible substructure are then modeled as grids of finite elements interconnected at nodes, and mass is either concentrated at the nodes or distributed throughout the element. As in the vehicle normal-mode formulation the deformations of the finite elements are described in terms of nodal coordinates. The equations of motion have the form:

$$M\ddot{q} + D\dot{q} + G\dot{q} + Kq + Aq = L \tag{8}$$

where M, D, and K are symmetric matrices and G, A, are skew-symmetric matrices, and L is the forcing function matrix. The matrix M is associated with the inertia properties of the vehicle; D is associated with damping; K is associated with the stiffness of the structure; and, G and A are associated with the spin properties of the vehicle. Unlike the vehicle normal-mode method, certain boundary conditions are applied which take into account the constraints of the flexible substructures.

The mathematical operations performed in the flexible vehicle analysis are applicable to the flexible appendages, that is, a first order modal equation can be written for each flexible substructure in the composite vehicle.

It is always the objective of the hybrid coordinate formulation to obtain a set of nonhomogeneous equations in terms of truncated modal coordinates for each flexible substructure which experiences large motions or nonlinearly controlled motions relative to a connected substructure. The substructure modal oscillations characterized by these equations will be driven not only by externally applied forces and torques, but also by the deviations of attached bodies from their nominal motions. It is, of course, necessary to combine each of the flexible appendage equations with additional equations written for the total vehicle, and for as many mixed groups containing both rigid and flexible substructures as required by the number of degrees of freedom in the system.

There are actually two different methods developed in hybrid-coordinate analyses. One method called synthetic-mode method employs equations of motion written separately for the rigid and elastic components of the vehicle while the typical hybrid-coordinate method explains the various ways in which the equations of motion of the total vehicle may be combined with appendage equations.

The material which is currently under study concerning hybrid-coordinate analysis has been presented by P. W. Likens.[4,6, 7]

The hybrid coordinate formulation is just now being applied to spacecraft[8]. In combining the good parts of both the discrete coordinate and vehicle normal-mode coordinate formulations, it is providing a very accurate and efficient means in describing the motion of nonrigid spacecraft.

III. Conclusions

The flexibility modelling techniques that have been surveyed are: (1) discrete coordinate formulation; (2) vehicle-normal-mode formulation; and (3) hybrid-coordinate formulation. The particular method used to analyze flexibility depends primarily on the particular spacecraft configuration.

If a configuration is simple enough to be described by only a small collection of rigid-bodies, the discrete coordinate formulation will provide an accurate description of the vehicle. The disadvantage of this method lies in the inability to model a complex spacecraft since a large number of rigid bodies would be necessary. Increasing the number of rigid bodies that model a spacecraft system increases the complexity of the problem as well as decreasing the efficiency of numerical integration programs to handle the high number of equations.

In preliminary design where linearization of the equations of motion are permitted, the vehicle normal mode formulation provides useful information. This method is restricted, however, to vehicles undergoing linear, elastic, small deformations and for systems which do not include nonlinearities, rotors, discrete dampers, or pronounced moving parts.

The hybrid coordinate formulation mixes the good parts of the other two types of formulation. It permits accurate simulation of complex modern space vehicles with a minimum number of coordinates.

IV. References for Appendix E

1. Hooker, W. W., and Margulies, G., "The Dynamical Attitude Equations for an n-Body Satellite," J. Astronaut. Sci., Vol. 12, pp. 123-128, 1965.

2. Likins, P. W., "Passive and Semi-Active Attitude Stabilizations-Flexible Spacecraft", Paper presented in AGARD lecture series No. 45 - "Attitude Stabilization of Satellites in Orbit", Brussels, 11-12 October and Stuttgart, 14-15 October 1971.

3. Hooker, W. W., "A Set of r Dynamic Attitude Equations for an Arbitrary n-Body Satellite Having r Rotational Degrees of Freedom," AIAA J., Vol. 8, 1970, pp. 1205-1207.

4. Likins, P. W., "Dynamics and Control of Flexible Space Vehicles," JPL TR 32-1329, Rev. 1, January 15, 1970.

5. Bisplinghoff, R. L., Ashley, H., and Halfman, R. L., Aeroelasticity, Addison-Wesley Publishing Co., Inc., Reading, Mass., 1955.

6. Likins, P. W., and Wirsching, P. H., "Use of Synthetic Modes in Hybrid Coordinate Dynamic Analysis", AIAA J., Vol. 6, pp. 1867-1872, 1968.

7. Likins, P. W., "Finite Element Appendage Equations for Hybrid Coordinate Dynamic Analysis", JPL TR 32-1525, October 15, 1971.

8. Likins, P. W., Marsh, E. L., Fleischer, G. E., "Flexible Spacecraft Control System Design Procedures Utilizing Hybrid Coordinates", JPL TM 33-493, September 15 , 1971.

APPENDIX F

Internal Autonomous Momentum Control Devices

(T. Edwards)

I. Introduction

Although detumbling by an external means is the ultimate goal of a rescue system, it may be desirable to have internal devices installed in the space vehicle which could detumble a disabled vehicle or, at least, lessen the tumbling motion until the rescue vehicle arrives. Such devices would become active upon loss of control and should be relatively simple, i.e., require little power, and be lightweight. Therefore, mechanisms are being studied to find possible candidates for internal devices to control or reduce tumbling. Also, methods of analyses for investigating these devices and the subsequent vehicle motions were surveyed.

II. Survey of Related Work

Devices for controlling tumbling can be broadly classified as active or passive. Active devices are those which use sensing instruments of some sort to command control torques. These systems require significant control logic and power. Typical active control mechanisms are mass expulsion and momentum exchange devices. One potential active control mechanism identified is the moveable mass system. By moving the control mass properly and changing the moments of inertia of the spacecraft, tumbling may be transformed into spin.

Passive devices may appear to be more attractive candidates in that they would require no onboard power or logic. Passive devices use the "wobbling" motion of the vehicle to activate simple mechanical or fluid devices which dissipate energy and lead to a simple spin state. Possible passive control systems identified are the viscous ring and pendulum dampers. Methods of modelling systems with passive control devices have also been surveyed.

III. Methods of Analysis

Active tumbling control devices are, perhaps, the simplest to formulate mathematically. The equations of motion are given by

$$\vec{T} = \frac{d}{dt} \vec{H}$$

where $\vec{T}$ is the torque acting on the spacecraft and $\vec{H}$ is the total angular momentum of the vehicle. The equations of motion that result are usually highly non-linear and require numerical solution.

For the analysis of passive damping control mechanisms, three techniques seem to be available. They are the energy-sink method, discrete parameter method, and the modal method.[1] For the energy sink method, the spacecraft is modelled as a rigid body and the damping mechanism is considered as an energy removal device or "sink". The assumption is made that the motions of the spacecraft actuate the damper, but the motions of the damper do not directly affect those of the spacecraft. Incremental changes in the kinetic energy of the system are calculated over one cycle and are used to compute an energy dissipation rate. Although this method is not rigorous, it can yield valuable estimates of spacecraft motion for vehicles using specific energy damping mechanisms which do not

involve large accelerations of mass relative to the spacecraft. The discrete parameter and modal methods are discussed in Appendix E.

IV. Discussion of Internal Devices

Mass expulsion systems for use as internal detumbling devices may be of monopropellant or bipropellant type. The monopropellant type appears to be more desirable since bipropellant systems tend to be heavier and more complex. The simplest means of orienting the thrusters is to place a pair of thrusters about each control axis. However, due to weight limitations this may not be possible, in which case it would be necessary to determine the number of thrusters needed and the best placement of these thrusters. One drawback of mass expulsion devices is that they require servicing and an onboard power supply, and for long term missions have questionable reliability.

Momentum-exchange devices have found many applications in the attitude control of satellites. The control scheme for momentum exchange devices is to store the unwanted tumbling motions of the spacecraft in the motions of the wheel. Typical momentum exchange systems are the three-axis reaction wheel and the double gimballed momentum wheel systems.[2] For such a system used as an internal device for detumbling, the system would be inactive during normal operations and would become active upon loss of control of the spacecraft.

The moveable mass system for control of tumbling has been suggested for a number of applications.[3,4,5] The concept is based on the assumption that the components of the spacecraft can perform relative motions and also, the system can be made to move as a quasi-rigid body, i.e., the components of

the spacecraft can be made to remain fixed relative to each other. The control scheme is to exploit the following fact. When the spacecraft moves as a quasi-rigid body the rotational kinetic energy, K, lies between two values determined by the constant angular momentum, H, and the maximum and minimum moments of inertia, I_{max} and I_{min}, respectively.

$$K_{min} = \frac{H^2}{2I_{max}} \leq K \leq \frac{H^2}{2I_{min}} = K_{max}$$

Thus, the control scheme is to make the control mass move relative to the spacecraft in such a way that K increases to K_{max} or decreases to K_{min} at which time the spacecraft will be in a simple spin state. Once a simple spin state has been reached, the spacecraft may be despun with another internal device or by an external device. A simple spin state would greatly facilitate crew escape and final detumbling by external means.

Passive dampers have been extensively discussed in the literature. One of these devices is viscous ring damper.[6] This device is desirable since it does not involve any moving parts, other than the fluid itself. The periodic accelerations and velocities of the tumbling spacecraft cause fluid motion and energy dissipation due to the viscous action of the fluid on the tube wall. Energy will be dissipated until the minimum energy state is reached in which case the spacecraft will be in a simple spin about its stable maximum moment of inertia axis. Another passive device, the pendulum damper, has been proposed for nutation damping of the NASA 21 Man Space Station.[6] The concept is similar to

that of the viscous ring damper except that the damping mechanism is a hydraulic dashpot activated by motions of a pendulum caused by vehicle tumbling. Passive damping systems must be investigated to determine if the systems can reduce the tumbling motions of a distressed vehicle to a flat spin state in a reasonable time. Once a flat spin state has been attained, yo-yo devices may be utilized to despin the spacecraft. Yo-yo devices are simple and effective but can only be used when the spacecraft is in a flat spin.

V. Conclusions

Several possible internal devices have been identified as possible choices for detumbing. These include both active and passive type devices. Mass expulsion and momentum exchange devices can completely detumble a spacecraft but the power requirements and weight penalties may be restrictive. The moveable mass concept and passive damping devices are simple but can only convert the tumbling motions into a flat spin state. Future tasks will involve simulation of the various control mechanisms identified and will aid in evaluating the relative merits and disadvantages of each mechanism.

VI. References for Appendix F

1. Likens, P. W., "Effects of Energy Dissipation on the Free Body Motions of Spacecraft," TR32-860, Jet Propulsion Lab., California Institute of Technology, Pasadena, California, July 1966.

2. Dougherty, H. J., Lebsock, K. L., and Rodden, J. J., "Attitude Stabilization of Synchronous Communications Satellites Employing Narrow-Beam Antennas," J. of Spacecraft. Vol. 8, No. 8, August 1971, pp. 834-841.

3. Childs, D. W., "A Movable-Mass Attitude-Stabilization System for Artificial-g Space Stations," J. of Spacecraft, Vol. 8, No. 8, August 1971, pp. 829-834.

4. Beachley, N. H., "Inversion of Spin-Stabilized Spacecraft by Mass Translation-Some Practical Aspects," J. of Spacecraft, Vol. 8, No. 10, October 1971, pp. 1078-1080.

5. Kane, T. R. and Scher, M. P., "A Method of Active Attitude Control Based on Energy Considerations," J. of Spacecraft, Vol. 6, No. 5, May 1969, pp. 633-636.

6. TRW Systems Engineering Mechanics Laboratory Staff, "Feasibility Study and Design of Passive Dampers for a Manned Rotating Space Station," NASA CR-163, March 1965.